JOVIAN AND COMPARATIVE ATMOSPHERIC MODELING

GARETH P. WILLIAMS

Geophysical Fluid Dynamics Laboratory/NOAA
Princeton University
Princeton, New Jersey

Princeton, New Jersey

1. INTRODUCTION

In this chapter, we describe the recent development of a Jovian meteorology and assess its impact on the evolution of comparative meteorology. The classical rationale for conducting comparative studies was given, long ago, by Edward Tyson (1651–1708), the founder of comparative anatomy, who wrote†

> Nature when more shy in one, hath more freely confest and shown herself in another. The anatomy of one animal will be the key to open several others, and until such time as we can have the whole completed 'tis very desirable to have as many as we can of the most different and anomalous.

† From "Anatomy of a Porpess." Tyson's studies of the porpoise—a mammal—also revealed the danger of classifying objects by their external appearance alone.

ADVANCES IN GEOPHYSICS, VOLUME 28A

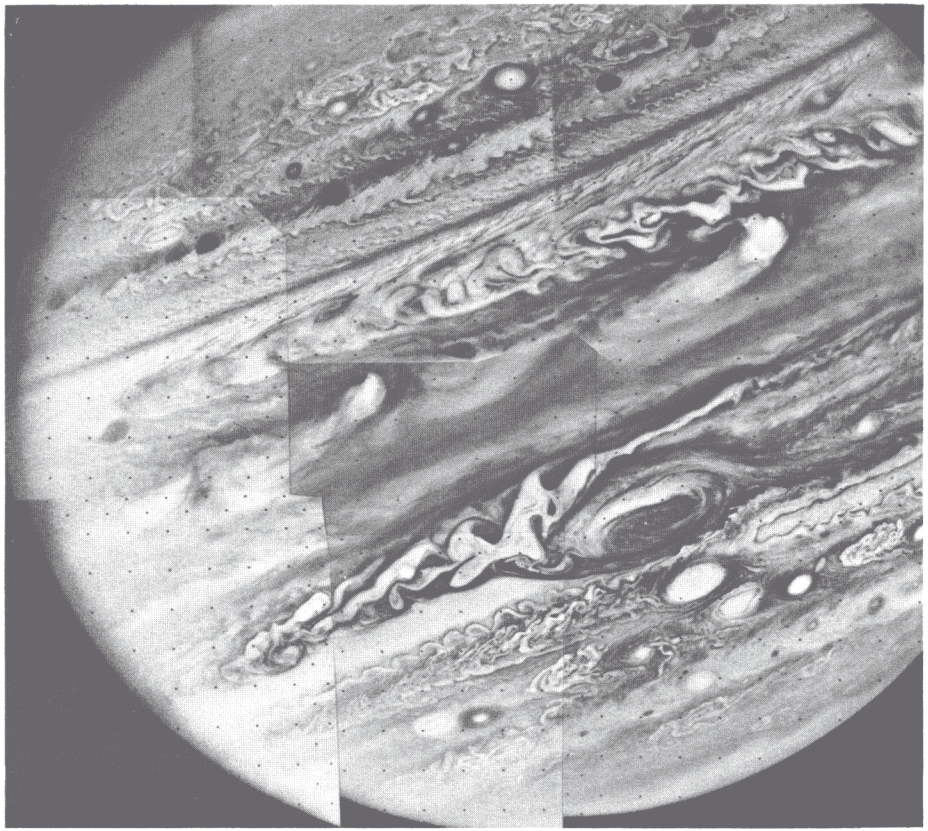

FIG. 1. A mosaic of Jupiter assembled from photographs taken through a violet filter by Voyager 1 in February 1979. A Large Oval passes just below the Great Red Spot while smaller ovals pass below it. Three plumes are apparent in the equatorial zone. Features as small as 150 km are resolved. (Photograph courtesy of Jet Propulsion Laboratory.)

1.1. Development of the Terrestrial Connection

1.1.1. Toward Unity. In the past decade, our view of Jupiter (and Saturn) has undergone a radical change. We no longer consider the Jovian circulation as being unique, steadily axisymmetric, and of uncertain dynamics but, rather, as a seething turbulent system with conventional meteorological processes at play and having close dynamical ties with Earth's atmosphere and oceans. These changes have been wrought mainly by theoretical developments in geophysical fluid dynamics (GFD), with high-resolution spacecraft measurements acting to substantiate the new view (Fig. 1.).

The pre-1975 theories all assume that some form of axisymmetric instability is responsible for the quasi-symmetric banded form of the circulation. All these theories had major defects — see Stone (1976) for their review. The modern GFD view of the circulation began when fundamental studies of planetary β turbulence revealed that zonally aligned flows are the preferred end state of eddy-driven quasi-horizontal nonlinear cascades on a rapidly rotating planet (Rhines, 1975; Williams, 1975a,b, 1978). Studies of quasi-geostrophic (QG) turbulence then showed that baroclinic instability could energize the eddies that drive the Jovian jets if the planetary baroclinicity $(\Delta T)_p$ (the isobaric pole-to-equator temperature difference) lies in the 5 – 60-K range (Williams, 1979a). These studies also showed that the energy decascade to larger scales barotropized the motions — particularly the jets — so that details of the vertical variation of the atmosphere (an unknown) may not be crucial to an understanding of the cloud-level circulation.

The QG studies also imply that in mid-latitudes Jupiter behaves like a larger, faster-spinning Earth (Williams, 1979b). Increasing the rotation rate in a global circulation model for Earth's atmosphere (ECM) produces powerful equatorial westerlies resembling Jupiter's, so the analogy also holds in the tropics (Williams and Holloway, 1982, 1985). Further calculations with the ECM suggest that Venus's circulation may have much in common with that of a very slowly rotating, diurnally heated Earth while Mars has connections with a moisture-eliminated Earth atmosphere. These analogies suggest that perhaps every planetary circulation has some elements that are universal and some that are unique. Physical generalities can compensate for observational deficiencies in developing an understanding of a particular planet.

While the Jovian planets are worthy of individual examination, the study of their connections with each other and with other rapidly rotating planets is vital to comparative meteorology. Such unity is sought mainly to simplify issues and to generalize the terrestrial paradigm but also because we prefer theories that connect hitherto unrelated problems. Meteorological similarities within the solar system could be merely coincidental (but convenient), or they could be intrinsic by virtue of a common planetary origin and

evolution (Pollack and Yung, 1980). Earth's atmosphere and oceans share a common GFD (Charney and Flierl, 1981), despite vast differences in their constituents, configurations, and thermodynamics, so there are already indications that disparate bodies can have a comparable dynamics.

All planets have special features that add individuality to their meteorologies: Venus has a dense cloudy atmosphere and a very slow rotation, Mars has a thin condensing atmosphere that exchanges mass with its polar caps, and Jupiter has an internal heat source and an indeterminate vertical structure. The main problem is to determine whether these factors provide merely a minor influence on the dynamics of the motion or whether they induce uniqueness. The movement toward a unified theory for the circulations of all planetary atmospheres and oceans is part of the credo of GFD (Pedlosky, 1979, p. 1; Charney and Flierl, 1981). The richness and complexity of Earth's atmosphere and oceans have led to concepts of such generality that they may suffice for explaining much that is seen on other planets.

The GFD view of the Jovian planets discussed in this article depends on the basic assumption that their atmospheres† are thin relative to their sublayers and are driven by differential solar heating. Theories based on this idea are successful in that they provide an explanation for the following aspects of Jupiter's motions: (1) the scale, amplitude, and zonality of the jets; (2) the scale, origin, waviness, and turbulence of the small eddies; and (3) the origin, longevity, form, anticyclonic bias, drift, scale and scale variations, uniqueness or multiplicity, and localization of the large coherent vortices—the Great Red Spot (GRS) and Large Ovals. All of these theories are mutually consistent and are also relevant to our understanding of Earth's atmosphere and oceans. We can thus claim to have a viable model of most of the major aspects of Jupiter's cloud-level circulation, one that has the full weight of meteorological principles behind it. These basic principles and their Jovian implications are discussed in detail in a companion review entitled "Circulation Dynamics" (hereafter CD85). In this paper, we concentrate only on modeling and observational developments and issues.

1.1.2. Unity or Uniqueness? Alternative views of Jupiter are still pursued. In particular, the classical view assumes that the planet is unique, that its atmosphere is thick and indistinguishable from its envelope, and that the motions are convectively driven, in astrophysical fashion, by internal heating (Busse, 1983; Ingersoll and Pollard, 1982). [See Iavorskaya and Belyaef (1983) for a review.] The main difficulties with this view are that to test it observationally requires probes that penetrate deep into the planet's interior and that modeling it requires a fundamental understanding of thermal tur-

† For convenience, we regard the "atmosphere" as being the solar-influenced, meteorologically active layer and the rest of the envelope as the "sublayer."

bulence. Neither is possible at present so the hypothesis has little practical value.

Linear analyses of the convection hypothesis are totally dependent on the eddy viscosity parameterizations of the thermal turbulence and so lack intrinsic significance. These formulations imply that alternating axisymmetric cylinders of motion exist throughout the planetary interior, extending from one hemisphere to the other (Busse, 1983). Motions at the tops of the cylinders are equated with the observed zonal flows. The analyses do not explain what determines the scale and amplitude of the jets or why the corresponding jets in opposite hemispheres differ. Neither do they explain the existence of the coherent vortices, the waves, and the turbulent eddies, nor their relationship to the jets. The idea of motions retaining their identity and momenta over the vast range of pressures in the planet's interior is difficult to justify. The convection hypothesis does not constitute a "model" of the circulation in the accepted sense of the term.

The real advantage of the thin atmosphere view has been in bringing Jovian studies into the mainstream of meteorological and oceanographical thought, to open them up to the powerful concepts and tools of GFD, and to make these planets relevant to terrestrial studies and comparative meteorology. The GFD view is simpler to pursue, generates richer possibilities, has a larger number of new consequences, and so can be tested more stringently. Conversely, to insist on the uniqueness of Jovian dynamics denies such advantages and condemns such studies to a meteorological pathology.

Before 1975, the real reason Jupiter was not understood was because Earth was not fully understood. If we had asked why Earth has only one (or two) jets per hemisphere, why the jets are azonal, and if we had systematically evaluated ECMs in parameter space, the Jovian connection would have been readily realized even though GFD theory was not then adequate for understanding the relationship. Reversing the usual rationale for planetary study, it is now clear that to understand Jupiter we need to understand Earth better.

1.1.3. Toward Coherence. Limitations in GFD theory also delayed our understanding of coherent vortices such as the Great Red Spot and Large Ovals. Resolution of this problem came finally from progress related to the study of long-lived ocean eddies. Jovian motions have much in common with oceanic ones: strong energy conversion by the small eddies, activity over a wide range of scales, weak dissipation, turbulent and coherent forms, and similar nondimensional parameter ranges. Differences occur not so much in the basic dynamical modes, but rather in their forcing mechanisms.

Initial developments in the modern explanation of the Jovian vortices began — when viewed with hindsight — with the suggestion (Golitsyn, 1970) that, because of the low dissipation level of quasi-horizontal motions in an unbounded atmosphere, the GRS could be a free vortex. The problem was to

explain how the rapid wave dispersion endemic to a rapidly rotating planet could be contained. One mechanism capable of balancing weak Rossby-wave dispersion is the weak nonlinear steepening provided by the meridional momentum transport induced by solitary waves in a latitudinal shear zone (Long, 1964). These Rossby shear-solitons have been applied to Jupiter (Maxworthy and Redekopp, 1976), but they differ from Jovian vortices in many ways: they are not oval in shape, they propagate very rapidly (Beaumont, 1980), they are weak vortices, and they have counter vortices lying beneath them (Flierl *et al.,* 1983).

No attempt has been made to simulate Rossby shear-solitons numerically so their stability and existence remains uncertain. Numerical studies of solitary Rossby waves were first made 30 years ago when they were first suggested as a cause of blocking (Yeh, 1949; Bolin, 1956). Those calculations indicated that quasi-geostrophic solitary waves disperse rapidly in a uniform environment but that divergence effects can greatly reduce the rate of dispersion, a result that has been recently exploited.

The early Jovian vortex theories conflict with the GFD view for the zonal circulation, which requires that quasi-geostrophic eddies be turbulent, not coherent, to drive the jets. It is not clear how turbulence and coherence can exist within the *same* dynamical regime. The resolution of this problem and the next development came with the realization that the Jovian vortices, because of their great size, are not quasi-geostrophic but lie in the divergence-dominated intermediate-geostrophic (IG) regime that occurs between the smaller QG and the larger planetary-geostrophic (PG) scales (see Section 3.2.1 for details). Long-lived, anticyclonic solitary vortices are the fundamental mode in the IG regime and occur readily at such scales. Nonlinear steepening of the fluid interface (or isotherms) balances dispersion in these solitary waves, which because they exhibit coalescence during collisions, not soliton behavior, are known as IG vortices or Rossby density-vortices (Williams and Yamagata, 1984; Williams and Wilson, 1985). Such vortices have also been produced in laboratory experiments (Antipov *et al.,* 1982).

When zonal currents become barotropically unstable at the IG scale, they produce solitary vortices in contrast to the periodic waves seen at QG scales. Just as the study of normal mode Rossby waves led to the discovery of barotropic instability, so has the study of solitary waves led to the discovery of the solitary instability (Williams and Yamagata, 1984). Thus the isolation of a vortex from its environment is no longer considered essential for vortex longevity. Jupiter's GRS and Large Ovals appear to be the Rossby vortices produced by weakly unstable zonal currents. Studies are now being made to determine whether solitary baroclinic instabilities can occur. Again, these discoveries could have been made 20 years ago by a systematic evaluation of simple models in parameter space.

Coherence and turbulence are thus seen to coexist by occurring at widely

separated scales. Barotropic and baroclinic instabilities coexist in the same way. Thus, small, turbulent QG-scale eddies, energized by baroclinic instability, drive zonal currents that can become barotropically unstable at the larger IG scale and produce coherent IG vortices that help equilibrate the jets.

1.2. Planetary Comparisons

1.2.1. Earth and Jupiter. The main problem in defining Jupiter's meteorology is that the nature and extent of the atmosphere and its motions are not known for the region below the clouds. Theories for the planet's interior [e.g., Stevenson (1982)] suggest that no solid surfaces exist except at great depth. It is in this absence of a lower surface that Jupiter's atmosphere differs most from Earth's atmosphere, while in its confinement of the motions by the thermal structure it most resembles the ocean.

Both atmospheres are partially heated from below, Jupiter by internal heating and Earth by surface heating due to atmospheric transparency to solar heating. Earth's winter hemisphere also experiences an internal heat source due to ocean storage. The primary interaction between atmosphere and ocean occurs in the tropics, where the ocean is statically stable and reacts more shallowly and rapidly and where the atmosphere is statically unstable and reacts more deeply and completely to convection. The distribution of the Jovian internal heat flux is unknown.

The sublayer heating on Earth produces small-scale moist convection that drives the lapse rate toward the moist adiabat. Jupiter's internal heat may also produce this effect, since there may be water clouds in the lower troposphere. Both atmospheres could thus be stable for large-scale processes. This stability could be enhanced by the baroclinic instabilities produced by differential heating. Above the tropopause, the stability is increased by the absorption of solar radiation by ozone on Earth and by methane and dust on Jupiter.

Both atmospheres experience a latitudinal gradient in solar heating. For Earth, baroclinicity levels are of the order of 30 K, while for Jupiter estimates vary from 3 to 30 K (Williams, 1979a; Branscome, 1982). The uncertainties occur because little is known about the absorption of solar heating below the clouds. Weak baroclinicities are effective in driving strong motions on Jupiter because they are associated with the gas constant for hydrogen, which is 14 times greater than the value for air; i.e., the gas is light.

These baroclinicities can produce single or multiple QG jets in the mid-latitudes of both planets (Williams, 1979a,b). On Earth, the mid-latitudinal jet overlaps the zonal flow associated with the Hadley circulation. On Jupiter, this overlap will be confined to a small region — if a Hadley circulation

exists—and the other QG jets will be unaffected. Regions of strong rising motion are usually confined to the hot towers of the Intertropical Convergence Zone (ITCZ) and determine the extent of the tropical region—30° latitude on Earth. A tropical regime may exist on Jupiter to about 10° latitude, but the form of a Hadley circulation in the absence of a lower surface is uncertain.

Separate heat sources in Earth's stratosphere produce a different type of circulation in that region, with large qualitative seasonal changes and a transfer of momentum and energy (by wave action) from the troposphere. On Jupiter, the absence of seasonal, topographic, and orographic forcing implies a simple stratospheric continuation of tropospheric motion, but convective forcing may induce some differences.

The turbulent eddies in both systems are due to baroclinic instability and they occur at the scale of the radius of deformation, $L_R = NH/f$. For Earth, the instability is of the Charney type and is greatly influenced by thermal gradients at the ground. For Jupiter, the instability is most likely to be that of the internal (Holton, 1975), interface (McIntyre, 1972; Simmons, 1974; Phillips, 1954), or unbounded (Dickinson, 1973) type. In the ocean, the simplest instabilities are of the Charney type, but mixed barotropic–baroclinic instabilities prevail in the Gulf Stream (Holland and Haidvogel, 1980). Ocean eddies, generated in the thermocline near the surface, penetrate into the deep ocean, where they generate currents (Holland *et al.*, 1984). Jovian eddies could act in this way and extend motions into regions well below those heated by the sun.

The terrestrial eddies have been identified by their statistical properties rather than by their linear characteristics [e.g., Gall (1976)]. A similar statistical identification of Jovian eddies has been attempted by Mitchell (1982). The radius of deformation is of 0(1000 km) for both atmospheres; for Jupiter, this is relatively small and produces nondimensional parameter values comparable to those given by $L_R \sim 0(100$ km) for the ocean. Numerical modeling of Jupiter and the ocean thus requires great resolution and computational power.

Coherent vortices occur in the ocean and on Jupiter at scales that are large relative to L_R. This scale separation does not exist in Earth's atmosphere to the same extent, and the only phenomenon of the same relative scale as the GRS is the Aleutian high [see Mahlman and Moxim (1978, Fig. 4.2)]. Whether blocking events are due to coherent vortices is unknown. Coherent vortices are less likely to occur in Earth's atmosphere because of strong dissipation in the boundary layer, unless they also have a strong energy source, as do hurricanes, for example.

Dissipation in the Jovian atmosphere can only occur through turbulent friction. Details of the dissipation mechanism are not important as its time

TABLE I. CLASSIFICATION OF PLANETS ACCORDING TO ROTATION RATE (OR PERIOD) AND OBLIQUITY[a]

Rotation rate (circulation type) Ω	Obliquity (degree of seasonal variation) θ_p		
	Low	Medium	High
Low (meridional)	Mercury[b] 0°, 59[d] Venus[c] 3°, −244[d]	Titan 27°, 16[d]	Pluto[b] > 50°, 6[d]
Medium (hybrid: meridional and zonal)		Earth 23°, 24[h] Mars[b] 24°, 25[h]	
High (zonal)	Jupiter 3°, 10[h]	Saturn[d] 27°, 10[h] Neptune[d] 29°, 15[h]	Uranus 82°, −15[h]

[a] From Williams and Holloway (1985).
[b] Seasonal variation enhanced by large orbital eccentricity.
[c] Circulation influenced by diurnal cycle.
[d] Seasonal variation reduced by interior heat source.

scale is relatively long, as in the ocean. This makes modeling simpler than for Earth's atmosphere where the planetary boundary layer must be dealt with, but it is nonetheless subject to the ambiguity of the subgrid closing parameterization. Changes in the Jovian jets are probably balanced by changes in the weak meridional cells and in the coherent vortices. Earth's jet is equilibrated by the transfer of momentum to the ground by the strong meridional circulation.

1.2.2. Saturn (Titan), Uranus, and Neptune. The other Jovian planets are considered to be essentially the same as Jupiter in structure and meteorology unless upcoming spacecraft encounters prove otherwise. [See Golitsyn (1979) and Trafton (1981) for details.] Jupiter, Saturn, and Neptune all have internal sources of heat of the same magnitude as their solar fluxes. This coincidence suggests that solar input controls the internal and meteorological heat transfers, not vice versa. Uranus has no internal heat source—perhaps because its extreme obliquity and seasonal variation have allowed the complete loss of internal energy via the unlit winter hemisphere. It is in their obliquities that the Jovian planets differ the most, Table I.

The radiative time scales† also differ greatly: 10 years for Jupiter and Saturn, 600 years for Uranus, and 2000 years for Neptune (Stone, 1973). These slow response times could insulate the atmospheres from seasonal changes or conversely limit dynamical activity to the uppermost regions.

† Ratio of thermal energy to solar heating flux.

The cloud-level circulation of Saturn exhibits multiple zonal jets that are stronger (400 m s^{-1} versus 100 m s^{-1}), wider, and more westerly in form than Jupiter's. These differences could be due to Saturn having a deeper atmosphere and to an inappropriate rotational reference frame. Saturn also displays coherent and turbulent eddies, though in less abundance or with less visibility. There is some evidence for bands on Uranus and for a tropical jet of 140 m s^{-1} on Neptune.

Titan, a satellite of Saturn, has an appreciable atmosphere. A slow rotation rate makes Venus its closest analog.

1.3. Modeling Problems and Strategy

A hierarchy of numerical models has been developed for terrestrial studies. According to Smagorinsky (1974) "the ultimate model of such a hierarchy could be conceived as one appropriate to any planetary atmosphere." In this section, we assess the planetary application of these models and the feasibility of developing a universal model.

1.3.1. Limitations. Direct simulations of nonterrestrial circulations have been realized for Mars (Leovy, 1979), Venus (Rossow, 1983), and Jupiter (Williams, 1979a). But it is not obvious that such modeling is justifiable in Jupiter's case. Given that we know only the cloud-level flow, is it really possible to develop an understanding of the atmospheric circulation? What sort of modeling is possible under these circumstances? What is the least level of observation below which we would be attempting the impossible?

The answer to these questions depends on whether Jupiter is unique or possesses universal characteristics. If the GFD paradigm applies, then there is no reason why we cannot use it to construct a reasonable range of possible descriptions of the complete circulation. For this we must assume a thin atmosphere. If we believe Jupiter is unique, then only extensive observation can reveal its nature and modeling is impossible at this time. We can proceed only because we believe general principles are at work.

The situation resembles, in some ways, the early stages of terrestrial studies in which efforts were made to construct circulation theories based only on ground-level data for the atmosphere and surface data for the ocean. Although those studies also had the advantage of knowing the baroclinicity and lapse rate for the atmosphere, they produced erroneous results. We have fewer data for Jupiter, but we now know better how the basic mechanisms work and how to avoid the main error of earlier studies — ignoring or underestimating the eddies. We proceed with optimism, but history suggests caution.

1.3.2. Model Types. For atmospheric and oceanic studies, numerical process and predictive (GCM) models have been found to be useful. Process models are simplified models that analyze the behavior of a single, idealized but complex (usually nonlinear) mechanism in isolation. An atmosphere or ocean contains many complex mechanisms. Process models allow us to determine the characteristics of each one and to estimate their relative importance. Basic process models are thus the first in a hierarchy of models that usually culminate in a comprehensive, synthesizing predictive model. Process models can thus help describe and reveal what happens in nature and in predictive models. Nothing is ever fully understood or explained; we achieve only levels of understanding or explanation. Process models provide the first and simplest level of such a hierarchy of explanations. Analytical models (e.g., turbulence closure theory) deepen our understanding of basic mechanisms. Idealized concepts provide a language for discussion rather than a true explanation. Modeling of Jupiter has been mainly at the process level.

Predictive models are for direct simulations, i.e., comparison with nature. They can be constructed when all the basic parameters and all the important complex processes are known. Such models are only possible for Earth, Mars, and perhaps Venus. They can also be used for comparative modeling to estimate how a representative atmosphere behaves when its parameters and physics are varied. Comparative modeling generates a large set of circulations that can be used to generalize terrestrial issues, to reveal analogs among planets, and to broaden the base from which to extrapolate. To date, such modeling has been limited to the evaluation of an ECM that, unfortunately, lacks universality in its vertical and sublayer structure. Earth's atmosphere and oceans present us with two quite different types of vertical structure to guide our ideas and prompt our imagination toward a more general conception.

1.3.3. Predictive Model Design. Process and comparative models have already given some indication of how a predictive Jovian circulation model (JCM) could be assembled. In particular, studies of β and QG turbulence reveal similarities between Earth and Jupiter in mid-latitudes, while comparative models reveal tropical connections. The similarities between the GRS and IG vortices only exist under conditions that place constraints on the vertical structure. Exploring the conditions under which the similarities and differences occur in greater detail could suggest a preferred vertical structure for the JCM. Thermodynamical modeling will require even greater ingenuity.

Circulation modeling began with the barotropic and quasi-geostrophic models of Charney and Phillips. These led to the primitive equation model of Smagorinsky, which in turn led to the development of the Mars and Venus

circulation models (MCM, VCM). The development at GFDL of a Jupiter circulation model (JCM) has followed the same systematic hierarchial evolution.

The construction of a JCM constitutes a major step in achieving the ultimate meteorological goal (Smagorinsky, 1974): the development of a general planetary model (GPM). To be dynamically universal such a model must be capable of describing either a semi-infinite or an unbounded atmosphere, but thermodynamical generality is harder to define. The high level of planetary observation, theoretical understanding, and computational power make such a model possible and worthwhile. It seems certain that all planetary models will be based on the pioneering ECM of Smagorinsky (1963) and its descendants.

2. Observations for Dynamical Modeling

For Jupiter and Saturn, some of the most basic items needed for dynamical modeling and verification are not available, but estimates are possible and are discussed below. Titan has a better-defined atmosphere and may be more easily modeled.

2.1. Stratification

2.1.1. Static Stability. The planetary scale dynamics of an atmosphere or ocean is primarily determined by the value and form of the Brunt Väisälä frequency $N(z)$, where $N^2/g = \theta^{-1}\theta_z = T^{-1}(T_z + \Gamma)$ is the static stability and Γ/c_p the adiabatic lapse rate (notation is standard unless defined). For planetary waves, the amplitude of N determines their scale while the form of $N(z)$ determines their vertical structure and their propagation characteristics. On Jupiter, motions could be trapped between a very stable stratosphere and a stable water cloud at the 5-bar level or, perhaps, by a stratification of the form $\operatorname{sech}^2 m(z - z_0)$ [cf. Pfister (1979)], where z_0 lies in the 1–5-bar region. Kinetic energy is confined to surface layers in the ocean by such distributions of $N(z)$ [e.g., Philander and Pacanowski (1980)]. Baroclinic instability cannot arise without wave trapping (Holton, 1974; Lindzen *et al.*, 1980), so its occurrence suggests the existence of appropriate forms of $N(z)$.

2.1.2. Clouds. Clouds have a major influence on the radiation balance and the formation of the stratification. In the most-accepted model of the gross vertical structure (Weidenschilling and Lewis, 1973), clouds form at three levels, a scale height apart, due to the condensation of ammonia, ammonia hydrosulphide, and water into ice crystals (Fig. 2). All are white

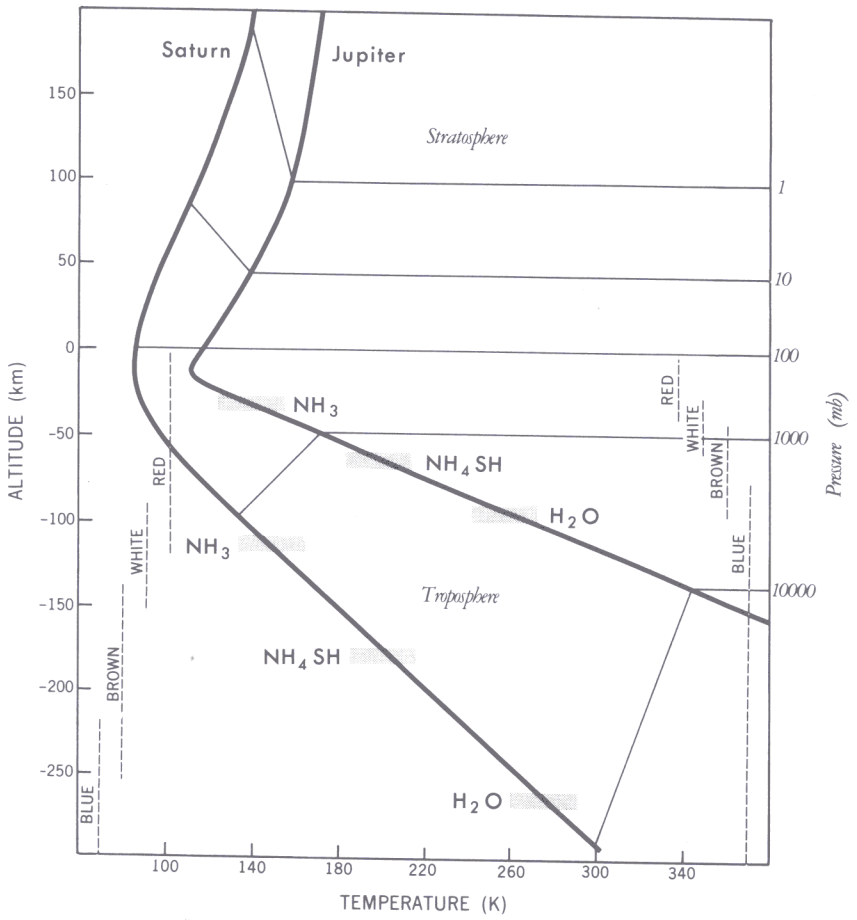

FIG. 2. Vertical profiles of temperature, cloud, and color for the upper atmospheres of Jupiter (on the right) and Saturn (on the left) as estimated from measurements in the radio and infrared wavelengths. [After Hunt and Moore (1982) and Hunt (1983).]

substances. The coloring is due to compounds of sulphur and phosphorus and depends on pressure, temperature, height, and latitude in a complex and poorly understood manner (Owen and Terrile, 1981) but may be approximately as shown in Fig. 2.

Most of the observed motions occur in the high ammonia cirrus clouds. The formation of the clouds may be attributed simply to geostrophic pressure variations (Williams, 1979a) or less simply to the vertical motions associated with the indirect (Ferrel) cells that equilibrate baroclinic jets (Williams and Holloway, 1985) and with direct (Hadley) cells. The first view is more consistent with the fact that the clouds disclose the horizontal motions

so directly, motions that easily overwhelm the weak updrafts expected on a rapidly rotating planet. On Saturn, the cloud albedo varies more weakly with latitude, which suggests that the cloud formation process is dynamically unimportant.

2.1.3. Lapse Rates. The hydrogen–helium mix of Jupiter and Saturn is sufficiently well known that their lapse rates, 1.9 and 0.9 K km^{-1}, and their scale heights, 22 and 38 km, may be considered accurate [e.g., Hunt (1983)]. In Fig. 2, the dry adiabatic lapse rate is used to yield an approximate temperature distribution below the ammonia clouds. In reality this distribution could be significantly modified through nonadiabatic heating by condensation, radiation, and convection. The major condensing gases are ammonia and water so latent heating could yield a moist adiabat in the lower atmosphere. The thermodynamical disequilibrium of the para and ortho forms of hydrogen at low temperatures could alter the specific heat c_p and influence the lapse rate (Conrath and Gierasch, 1984). Above the ammonia clouds, observations in the radio and infrared frequencies reveal a tropopause and a highly stable stratosphere (due to absorption of radiation by methane and haze).

In the theoretical cloud models, the strongest stratification occurs in the water cloud and most of the radiation is absorbed in the region above it, so it is not unreasonable to expect deviations in the lapse rate of up to 10% from the dry adiabat in the troposphere. Such values ($\theta_z = 0.2$ K km^{-1}) can be observed just above the clouds (Lindal *et al.*, 1981) and give $N^2 \sim 3 \times 10^{-5}$ s^{-2} (as in the ocean) and $L_R \sim 1000$ km (as in the waves). In the lower stratosphere, values of $N \sim 5 \times 10^{-4}$ s^{-2} and $L_R \sim 400$ km are suggestive of smaller-scale waves but these have not been detected (Branscome, 1982).

2.2. *Baroclinicity and Barotropy*

2.2.1. Heat Sources. The brightness temperatures of Jupiter and Saturn, 124 and 94 K, reflect internal heat sources that are $\frac{2}{3}$ and $\frac{4}{5}$ of the solar input. These source values are substantially smaller than earlier estimates (Hanel *et al.*, 1983). The latitudinal distribution of the internal heat flux at the base of the atmosphere is unknown and is not necessarily uniform. This heat source, like that of Earth's ocean, reduces the imbalance in the solar heating but is unlikely to completely eliminate the need for meridional atmospheric transport. Our lack of knowledge about the value of $(\Delta T)_p$, the baroclinicity, below the clouds poses a major modeling problem.

2.2.2. Global Temperature Variation. The observed latitudinal and longitudinal variations in the infrared brightness temperature relate to thermal emission from above the ammonia cloud decks. For Jupiter, they indicate a cloud-level temperature difference $(\Delta T)_{CL}$ of 5 K between high and low latitudes. Local variations are also about 5 K at the cloud top (800 mb) and at the tropopause (150 mb) and they have some correlation with the visible features, i.e., the albedo. For example, the GRS is slightly cooler and therefore higher than its environment (Hanel *et al.*, 1979). For Saturn, seasonal variations result in a $(\Delta T)_{CL}$ of 10 K in the Northern (winter) Hemisphere and a much smaller value in the Southern Hemisphere (Conrath and Pirraglia, 1983). Longitudinal variations of 1 to 2 K reflect eddy activity in both planets.

2.2.3. Baroclinicity Estimates. It is unlikely that the observed (nonisobaric) temperature differentials $(\Delta T)_{CL}$ are an accurate indicator of the baroclinicity below the clouds. Although baroclinicities of 5 K are sufficient for energizing an atmosphere with a weak dissipation and a large specific heat, it is likely that larger values occur. On Earth, the $(\Delta T)_p$ of the lower troposphere is much larger than the ΔT along the tropopause. The small values of $(\Delta T)_{CL}$ on Jupiter could be due to variations in cloud height: if the clouds in high latitudes are a half-scale height lower than those near the equator, then a $(\Delta T)_p \sim 30$ K ensues (Gehrels, 1976). If the polar region receives only internal heat while the equatorial region gets both internal and solar heat, then $\Delta T \sim 30$ K is predicted. So far, it has not been possible to narrow the estimated baroclinicity range of 5–30 K.

2.2.4. Thermal Wind Fallacies. The main diagnostic tool used—and misused—to probe below the clouds is the thermal wind relationship

$$\hat{\mathbf{v}} = \mathbf{v}(p_2) - \mathbf{v}(p_1) = \frac{R}{f} \ln \frac{p_1}{p_2} \mathbf{k} \times (\nabla \tilde{T})_p \tag{2.1}$$

where $\tilde{(\cdot)}$, $\hat{(\cdot)}$ denote the barotropic and baroclinic components. This connects the winds at two pressure levels with isobaric variations in the vertically averaged temperature $\tilde{T}$ using the geostrophic and hydrostatic relationships

$$\mathbf{v} = \frac{1}{f} \mathbf{k} \times (\nabla \Phi)_p, \qquad \Phi(p_2) - \Phi(p_1) = R \ln \frac{p_2}{p_1} \tilde{T} \tag{2.2}$$

respectively [e.g., Houghton (1977, p. 80)]. The thermal wind relationship has been used in two ways: (1) to estimate the depths of the Jovian atmospheres using the observed cloud-level velocities and temperatures $\mathbf{v}_{CL}$ and

T_{CL} (Lorenz, 1953; Smith *et al.*, 1982) and (2), inversely, to estimate the flow below the clouds using the observed T_{CL} and a presupposed depth (Conrath and Pirraglia, 1983; Flasar *et al.*, 1981b). Such applications are fraught with danger and error and are the cause of much misunderstanding.

All applications of the Eq. (2.1) set $\mathbf{v}(p_2) = \mathbf{v}_{CL}$, and assume that $\mathbf{v}(p_1) = 0$ at a so-called "level of no motion." This representation of the baroclinic component of the wind $\hat{\mathbf{v}}$ is only meaningful when $\hat{\mathbf{v}}$ is fairly uniform and is comparable with or larger than the barotropic component $\tilde{\mathbf{v}}$. The application of the thermal wind relation gives meaningless results if the motions are predominantly barotropic, which they are in weakly dissipative systems such as the ocean and Jupiter, where it is possible for weak baroclinicities to pump up large quasi-barotropic currents with $\tilde{\mathbf{v}} \gg \hat{\mathbf{v}}$ [e.g., Williams, (1979a, Fig. 8)]. Then $\mathbf{v}_{CL}$ indicates $\tilde{\mathbf{v}}$, not $\hat{\mathbf{v}}$. It should be noted that oceanographers have recently realized the error of this approach: "One regrets that the barotropic field was for so long obscured as a level of no motion" (Rhines, 1979). The problem can be overcome using the β-spiral method (Stommel and Schott, 1977), but this requires temperature data in the vertical and horizontal directions. These criticisms also apply to analyses based on the cyclostrophic wind relation.

Applications of the geostrophic relation [Eq. (2.2)] to Saturn's cloud-level winds have also been misinterpreted. When the relation is integrated over latitude, it produces a large value for the pole-to-equator gradient in the geopotential height $\Delta\Phi$. However, $\Delta\Phi$ is also a measure of the net angular momentum, which for a weakly dissipative atmosphere should be very small. This contradiction implies that the reference frame used in defining the (excessively prograde) winds is incorrect [cf. Allison and Stone (1983)] and that the tropical jet is strongly baroclinic. It does not imply that the atmosphere is very deep [cf. Smith *et al.* (1982)].

2.2.5. Evidence for Barotropy. The fact that the Jovian jets are so stable and so constant suggests that they are predominantly barotropic and thus have great inertia to baroclinic changes. Weak baroclinicity is only influential if it acts for a long time. Barotropy is also suggested by the close relationship between jet widths and bands via the expression produced by barotropic β-turbulence theory, $L_\beta = (U/\beta)^{1/2}$, where U is the velocity scale. Such jets could penetrate to a depth of $h_\beta = (f/N)L_\beta$ while baroclinic eddies penetrate to $h_R = (f/N)L_R$ [cf. Holland *et al.* (1984)]. Assuming possible values of $N^2 = 3 \times 10^{-5}$ s^{-2}, $L_R = 1000$ km, and $L_\beta = 5000$ km gives $h_\beta = 200$ km and $h_R = 40$ km. The Phillips criterion for baroclinic instability requires a critical shear of $\hat{u} = \beta L_R^2$, which equals 1 m s^{-1} per scale height and implies that $\hat{u} \ll \tilde{u}$. Thus in a weakly dissipative system the barotropic components

of the circulation could be substantially stronger, wider, and deeper than the baroclinic ones.

2.3. *Cloud-Level Circulation*

2.3.1. Rotation Rate. In defining the cloud-level circulation, ambiguities arise due to uncertainties as to which rotating reference frame is the most appropriate and as to which height the cloud-tracked winds refer. The latter problem is not serious if the winds are strongly barotropic. However, the observed motions define a very relative circulation.

The customary rotation rate is based on the radio frequency and gives velocities relative to the so-called System III reference frame. However, the bulk of the planet (and its magnetic field) need not rotate at the radio frequency. In addition, dynamical models of the GRS and Large Ovals suggest that these vortices are moving more rapidly westward by 5 to 15 m s^{-1} than System III implies (Williams and Yamagata, 1984), while the observed prograde bias in Saturn's jets suggests that the winds be made 70 m s^{-1} more easterly to achieve momentum balance. These problems indicate that reference frames — say System IV — with rotation periods that are about 1 min and 5 min shorter than System III be used for Jupiter and Saturn.

2.3.2. Jets and Bands. The high-resolution zonal winds obtained from tracking cloud features as small as 100–200 km over short time intervals (about 1 day) in Voyager spacecraft data have essentially the same structure (Fig. 3) as the winds derived from Earth-based tracking of larger clouds over lengthy periods. Now, however, the finer details of the motions, the rapid variations of the turbulent eddies and their interactions with the coherent vortices can be followed in remarkable detail for both Jupiter (Beebe *et al.*, 1980; Ingersoll *et al.*, 1981; Limaye *et al.*, 1982) and Saturn (Smith *et al.*, 1982; Sromovsky *et al.*, 1983).

The Voyager data indicate that the amplitudes of the jets are somewhat greater than originally thought but that the amplitudes vary little in time. The observations also reveal that alternating easterly and westerly jets, with amplitudes of up to 20 m s^{-1}, extend as far as 72° latitude (the observational limit) in both hemispheres (Beebe, personal communication, 1984) — even though cloud banding ends at 45° latitude. The jets are fairly symmetric between hemispheres but the bands are not, and the latter provide a more sensitive measure of temporal variations.

The bands (color, albedo) of Jupiter have changed continuously over the years. Between the Pioneer and Voyager encounters, a period of 4 years, one

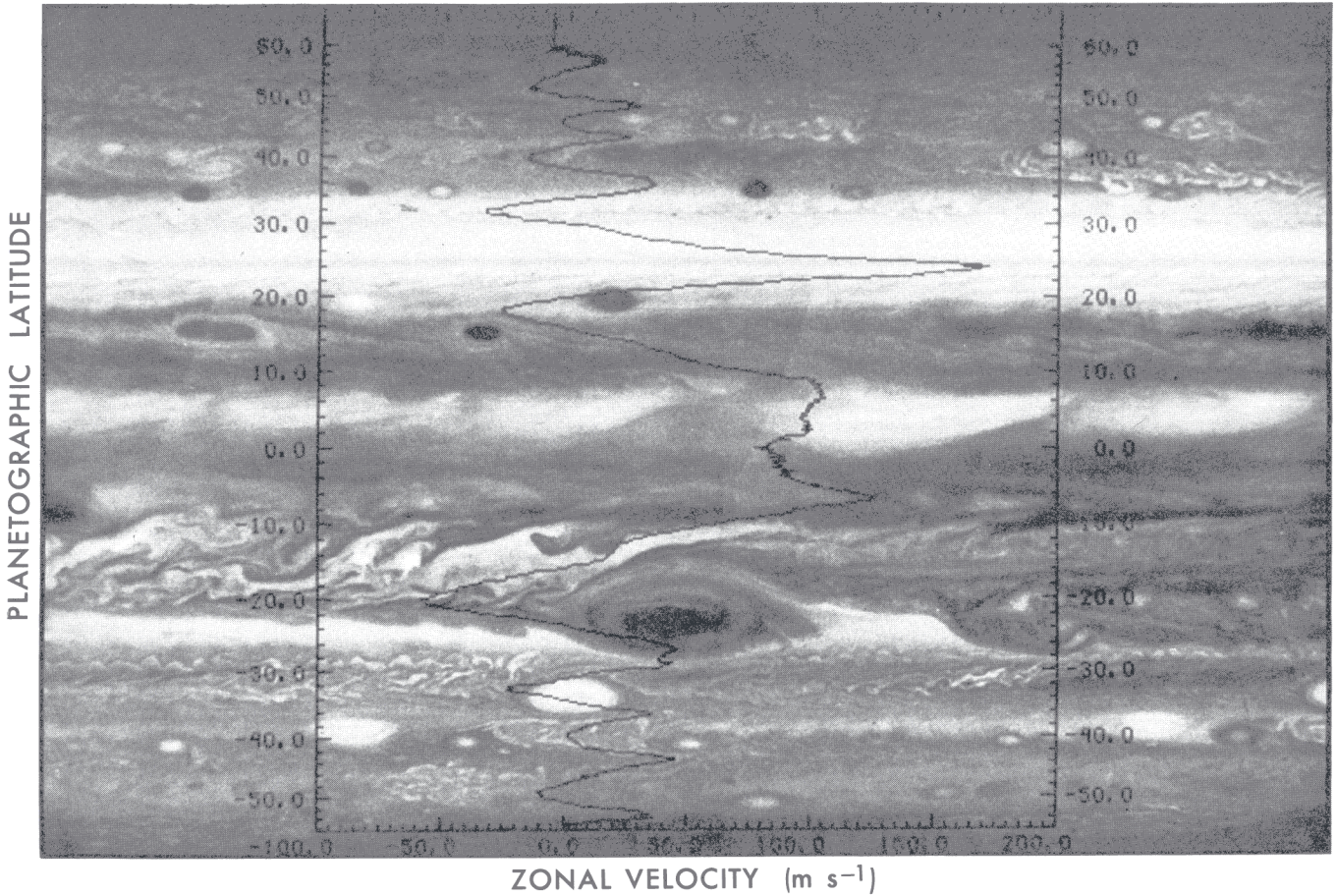

FIG. 3. Latitudinal profile of the mean zonal wind relative to System III, estimated from Voyager 2 cloud tracking. [Prepared courtesy of S. S. Limaye (1985).]

zone doubled in size and another halved. But during the two Pioneer encounters (1 year apart) there was little change in cloud structure. Bands appear to vary significantly with periods of 4 to 5 years but occasionally change in only 1 year, reflecting perhaps different phases of an energy cycle.

The correlation between the unchanging jets and the variable bands is thus not as simple as once thought. On Jupiter, there is still a reasonable correlation between the zonal motion and the bands, with jet maxima coinciding with belt–zone interfaces; but, on Saturn a correlation exists only for the mid-latitudinal jets, with extrema coinciding with the centers of the bands (Smith *et al.*, 1982). However, the correlation between temperature variations near the tropopause and the visible markings of Jupiter is clearcut (Hanel *et al.*, 1979). All of these relations are consistent with the idea that the jets are predominantly barotropic while the bands depend more on baroclinic factors.

2.3.3. Eddies and Vortices. Spacecraft observations have revealed the flow fields inside the long-lived, coherent vortices — the GRS, Large Ovals, and Small Ovals — that occur at latitudes 22°, 33°, and 41° (Mitchell *et al.*, 1981). These anticyclonic eddies are all very similar in form, environment and parameter values. They are strong vortices: the relative vorticity of the GRS exceeds the ambient vorticity by a factor of 4 and wind speeds exceed 100 m s^{-1} near the periphery. Flow is along closed symmetric ellipses so interaction with the zonal flow is limited. Between the two Voyager encounters (5 months) considerable changes occurred in the flow just west of the GRS and resembled the breaking of a PG-scale planetary wave.

In contrast to the Large Ovals, the GRS appears to have its vorticity concentrated near its outer boundary and to possess a quiescent interior. These differences could be due to the greater size of the GRS (Williams and Wilson, 1985), or, alternatively, the variations could be due more to vertical shears in the winds than to real differences in horizontal structure, especially if the winds peak at the height of the peripheral clouds and decay above it. There is no direct evidence of organized vertical motion within the vortices.

The GRS has been observed since the invention of the telescope and the Large Ovals since their birth in 1938. The formation of the Large Ovals is well documented — they took 15 years to develop into strong vortices — and is consistent with the behavior of weak barotropic instability at the IG scale (Williams and Wilson, 1985). Both the GRS and Large Ovals have contracted in longitude, the former from 40,000 to 24,000 km in this century. According to theory, this indicates increased amplitude and steepening, as energy is extracted from narrowing jets, and not vortex decay.

The longitudinal drift of the GRS has varied over the past 150 years, changing direction every 50 years in System III coordinates. On top of its

recent drift at 5 m s^{-1}, the GRS oscillates in longitude with an amplitude of 0.9° and a period of 90 days (Solberg, 1969). According to theory, such variations could be related to changes in vortex amplitude, current amplitude, or the radius of deformation. However, theoretical vortices only propagate westward, so changes in direction in System III really indicate changes in speed in System IV.

Persistent coherent cyclonic eddies also occur. In the Southern Hemisphere (Mitchell *et al.,* 1979), they are induced in cyclonic shear regions by the GRS and Large Ovals. In the Northern Hemisphere at 14° latitude, the cyclonic "barges" (Hatzes *et al.,* 1981) are primary vortices that drift eastward at 2 to 5 m s^{-1} in System III. According to theory, cyclonic vortices are long-lived only when they lie in a strong easterly flow. The flow at 14°N could be easterly if averaged vertically in System IV.

Disturbances peculiar to the tropics are the so-called "plumes" that form the centers of a wavelike train of features moving with the 100 m s^{-1} westerly jet at 10°N (Fig. 1). Some plumes are brighter and more structured than others and have been described as "active convective centers," 1000–2000 km long (Hunt and Müller, 1979; Hunt *et al.,* 1981, 1982). Smaller (gravity?) waves are seen in the tails of the plumes. The tropical wave containing the plumes has the same scale as the GRS and could be generated by disturbances emanating from that vortex. Because of its size, the GRS can generate waves capable of propagating beyond the critical latitude at 10°S but which would be trapped at 10°N [cf. Williams and Yamagata (1984, Fig. 8)]. It seems unlikely that wave-CISK—which requires low ventilation rates for moisture accumulation (Grey, 1978)—could arise in such rapidly moving currents, especially in latitudes in which the downward branch of a Hadley cell might occur.

Saturn's eddies resemble Jupiter's in form and behavior but are generally smaller and shorter lived (Sanchez-Lavega, 1982; Sromovsky *et al.,* 1983). At the Voyager encounter, three brown Ovals with diameters of 5000 km existed at 42°N and a solitary 10,000 km Oval existed at 72°N. The complex interaction of two small white vortices was observed in fine detail (Sromovsky *et al.,* 1983) and it more closely paralled the oblique collisions of IG vortices [cf. Williams and Yamagata (1984, Fig. 10)] than the collisions of the vorticity concentrations generated by turbulence (McWilliams, 1984).

Disturbances said to be peculiar to Saturn may just be poorly resolved vortices (Sanchez-Lavega, 1982). These so-called Great White Spots have occurred 5 times in 80 years with diameters as large as 25,000 km in both the tropics and mid-latitudes. More than one type of vortex may be involved. Their lives are short (months). They sometimes expand longitudinally to fill the whole zone and generate other spots, actions consistent with the development of barotropic instability (Williams and Wilson, 1985). The "ribbon

wave" observed at 46°N, with cyclones to the north and anticyclones to the south, is suggestive of barotropic instability at the QG scale [cf. Williams and Yamagata (1984, Fig. 17)]. A similar, but nonwavy, thin brown line or ribbon occurs in the center of a similar westerly jet at 25°N on Jupiter and could be a barotropically stable version of such cloud formation.

2.4. *Data Analysis*

2.4.1. Quasi-Geostrophic Instabilities. The necessary condition for the instability of zonal flows involves the potential vorticity gradient, which for QG scales, can be written as

$$q_y = \beta + \tilde{q}_y + \hat{q}_y, \qquad \tilde{q}_y = -\tilde{\bar{u}}_{yy}, \qquad \hat{q}_y = -\hat{\bar{u}}_{yy} - \frac{1}{\rho_s}\left(\frac{\rho_s}{S}\hat{\bar{u}}_z\right)_z + \frac{\hat{\bar{u}}_z}{S}\delta \quad (2.3)$$

where δ denotes interface contributions.

Estimates of the barotropic term $\beta + \tilde{q}_y$ using cloud-level winds are error prone as the winds may not give a good measure of the vertically averaged flow, and their second derivatives cannot be accurately calculated. One set of estimates from Voyager data suggests that Jupiter's jets are mildly barotropically unstable or mildly baroclinic (Ingersoll *et al.*, 1979; Mitchell *et al.*, 1981), while a second set suggests that all easterly jets are strongly unstable or strongly baroclinic (Ingersoll *et al.*, 1981; Limaye *et al.*, 1982). Although both hemispheres appear to be equally unstable (or baroclinic), the coherent vortices generated by barotropic instability only occur in the Southern Hemisphere (SH). This suggests that either (1) the SH is marginally unstable and the Northern Hemisphere (NH) marginally stable or (2) the instabilities are in the shear zones in the SH but in the jet maxima in the NH and hence less visible, except as ribbon waves (see Section 2.3.3). For Saturn, the noise level in the winds precludes meaningful estimates of $\beta + \tilde{q}_y$ [cf. Smith *et al.* (1981) and Sromovsky *et al.* (1983)].

The QG form of $\tilde{q}_y$ is not really appropriate for Jupiter, given the large scales of the jets. At such scales, divergence effects due to the displacement of free surfaces shared with deeper underlying or overlying layers are important and instability depends on the expression $\beta - \tilde{\bar{u}}_{yy} + (\tilde{\bar{u}}/L_D^2)$, where L_D is the external radius of deformation (Lipps, 1963). This criterion has not been estimated for the data.

In the barotropic β-turbulence theory, jets generated by *homogeneous* forcing attain a state of neutral stability with $\tilde{\bar{u}}_{yy} = \beta$ (Rhines, 1975). In a baroclinic atmosphere, forcing by baroclinic instabilities (in the jet maxima) is inhomogeneous and can produce barotropically unstable jets. Thus the two forms of instability can coexist, at vastly different scales L_R and

L_β [cf. Brown (1969)]. Estimates of the eddy energy conversion (Section 2.4.2) fail to discriminate between opposing contributions at the two scales and appear to be dominated by the more easily measured small-scale components.

The baroclinic term $\hat{q}_y$ is significant if the ratio $\alpha = f^2 u_{zz}/\beta N^2$ is large. If we chose $u_{zz} \simeq u_z/\mathrm{H}$ (to avoid the errors noted in Section 2.2.4), then $\alpha = h/H$, where $h = f^2 u_z/\beta N^2$ is the eddy penetration scale (Held, 1978). The shear u_z can be estimated from thermal data for the upper troposphere, where a close correlation between u_z and u indicates that most jets gain strength below the clouds (Pirraglia *et al.*, 1981). The observations give $u_z H = -10\ \mathrm{m\ s^{-1}}$, $N^2 = 3 \times 10^{-5}\ \mathrm{s^{-2}}$ and thence $\alpha = 5$. So subcloud baroclinic instability is indicated.

2.4.2. Kinetic Energy Conversion. The equation for eddy kinetic change in a barotropic fluid is best written as

$$\overline{K'_t} = C_1 - (\overline{v'p'} + \overline{v'K'})_y$$

where $K'(y) = \bar{u}u' + \frac{1}{2}(u'^2 + v'^2)$ and $C_1(y) \equiv \bar{u}(\overline{u'v'})_y$. According to the nonacceleration theorem, these forms of the conversion and flux divergence terms are preferred over those in which the conversion term is written as $C_2(y) \equiv -\overline{u'v'} \cdot \bar{u}_y$. This is because only the former are identically zero for a steady wave propagating in a sheared environment and so only they are locally meaningful. With the first forms the error of identifying regions in which $C_2 > 0$ and $(\overline{v'p'})_y > 0$ as barotropically unstable can be avoided.

Several evaluations of the expression $C_2(y)$ have been attempted that use Voyager cloud-level winds observed over a 30-hr interval. Such estimates are useful provided no local (in latitude) or climatological significance is attached to them. One set of estimates (Beebe *et al.*, 1980; Ingersoll *et al.*, 1981), in which the cloud-level winds are assumed to penetrate to the 2.5-bar level, produces large positive values of C_2 that imply the mean flow will double or be replenished in 3 months by using 10% of the solar energy input. This unrealistic result suggests that the estimates are inaccurate. A second set of estimates (Limaye *et al.*, 1982) eliminates the systematic sampling errors of the first (by using lower resolution) and yields $C_2 \simeq 0$. A third estimate (Mitchell, 1982), using uniform sampling and high resolutions, again gives large positive values of C_2.

Thus there are contradictory indications that the eddies occasionally supply energy to the mean flow at cloud level, but there are no estimates of behavior in the more important lower atmosphere. Oceanographic evaluations of local energy balances have also been interpreted as indicating that the Gulf Stream is accelerated by the eddies. However, the cross-stream-averaged value of $\overline{u'v'} \cdot \overline{v_x}$ is nearly zero, so such results may indicate the

transfer of energy from one side of a jet to the other and not mean flow generation [cf. Charney and Flierl (1981, p. 507)].

2.4.3. Equilibrium and Dissipation. There are three possible mechanisms for jet equilibrium: (1) dissipation by gravity waves or by exchanges with the sublayer, (2) loss of energy to the coherent vortices by barotropic instability, or (3) balance by the induced meridional circulation. The momentum equation

$$-f\bar{v}_a + (\overline{u'v'})_y = D \tag{2.4}$$

summarizes these effects at the quasi-geostrophic level, where v_a is the ageostrophic flow. Observations give no clue as to which process prevails, if any.

The dissipation mechanism operates in Earth's stratosphere and if we adopt the stratospheric dissipation coefficients (Schoeberl and Strobel, 1978) a dissipation time scale of 900 days is predicted (Branscome, 1982). This value is consistent with our suggestion that there is a wide separation between the dynamical (50-day) and dissipative time scales. Equilibration by mechanism (2) requires a balance between the baroclinic eddy source term $[(\overline{u'v'})_y]^{L_R}$ and barotropic eddy loss term $[(\overline{u'v'})_y]^{L_\beta}$, where brackets denote averaging over scales close to L_R or L_β. The absence of coherent vortices in many regions suggests this is not the main control process. No estimates of the scale dependence of the eddy conversion have been made.

With mechanism (3), a meridional circulation of about 0.1 m s^{-1} could balance the eddy fluxes estimated by Mitchell (1982). Thus the cells would be much weaker than those of Earth's atmosphere, and if they are primarily induced by baroclinic instability, they would be confined to the jet extrema and be narrower than the jets ($L_R \ll L_\beta$)—as are some of the bands. There may be no meridional circulation in the region between these cells. Estimates of the mean meridional wind $\bar{v}$ from Voyager data produce values of about 1 m s^{-1}, but these cannot be accurate given that the rms winds have values up to 10 m s^{-1}.

2.4.4. Spectra. Spectral analyses of the Voyager cloud-level winds produce such noisy spectra that it is impossible to detect a simple wave number relationship of the form k^{-n}, although—like for Earth—a k^{-3} result has been claimed (Mitchell, 1982). The best indication of the nature and dimensionality of the nonlinear exchanges is the close relationship between jet widths and amplitudes via the L_β expression of β turbulence. The steadiness of the jets also reflects the barotropization associated with β-turbulence effects.

Recent numerical studies of two-dimensional and β turbulence (see CD85) yield spectral slopes with powers ranging from $n = 3$ to 6 in the

enstrophy cascading scales, with the actual value depending on the forms of the forcing and dissipation. The absence of simple turbulence behavior makes data interpretation very difficult.

2.5. *New Worlds: Titan*

2.5.1. Significance. A bonus from the spacecraft encounters is the discovery that Titan, Saturn's largest satellite (2575-km radius) has a substantial (1.6-bar) nitrogen atmosphere and perhaps a methane ocean (Smith *et al.*, 1981, 1982). Clearly Titan is a planet of physical relevance to terrestrial studies and possesses great modeling potential. The planet has dynamical relevance for Venus because of the length of its rotational period (15.9 days) and for comparative meteorology it is an invaluable addition to the meager category of slowly rotating systems.

2.5.2. Stratification. The atmosphere has observed temperatures of 94 K at the surface, 71 K at the tropopause level (43 km, 140 mb), and a 170-K limit in the upper stratosphere (200 km) (Fig. 4) (Lindal *et al.*, 1983). With $g = 135$ cm s^{-2}, the scale height is 18 km. The lapse rate has the adiabatic value for dry nitrogen, 1.4 K km^{-1}, only near the surface and drops sharply to 0.9 K km^{-1} at the top of the boundary layer (3.5 km). Methane makes up 1% of the atmospheric mass but its moist adiabat, 0.3 K km^{-1}, is not observed so saturation is absent. There are methane clouds in the troposphere and an aerosol layer plus two haze layers in the stratosphere (Samuelson *et al.*, 1981, Fig. 2; Smith *et al.*, 1981, 1982). Carbon dioxide is another important minor constituent (Samuelson *et al.*, 1983).

2.5.3. Global Temperature Variation. The observed brightness temperatures indicate pole-to-equator temperature differences of 3 K near the surface, 1 K at the tropopause, and 20 K in the stratosphere (at 0.3 mb) (Flasar *et al.*, 1981a). Hemispheric asymmetries occur in the stratospheric temperatures due to seasonal effects, but no diurnal effects have been detected. The radiative time scale thus exceeds a Titan day in the stratosphere and reaches an estimated 140 years in the troposphere.

Ground-based observations have revealed dramatic seasonal variations in the planet's overall appearance [cf. Sromovsky *et al.* (1981)]. If the troposphere is involved, the efficient dynamical heat transports of the Hadley cell that occurs at low rotation rates could be important to these secular albedo changes.

2.5.4. Circulation. Visually, Titan is bland because of the opaque stratospheric hazes. No surface or cloud features have been seen so there are no

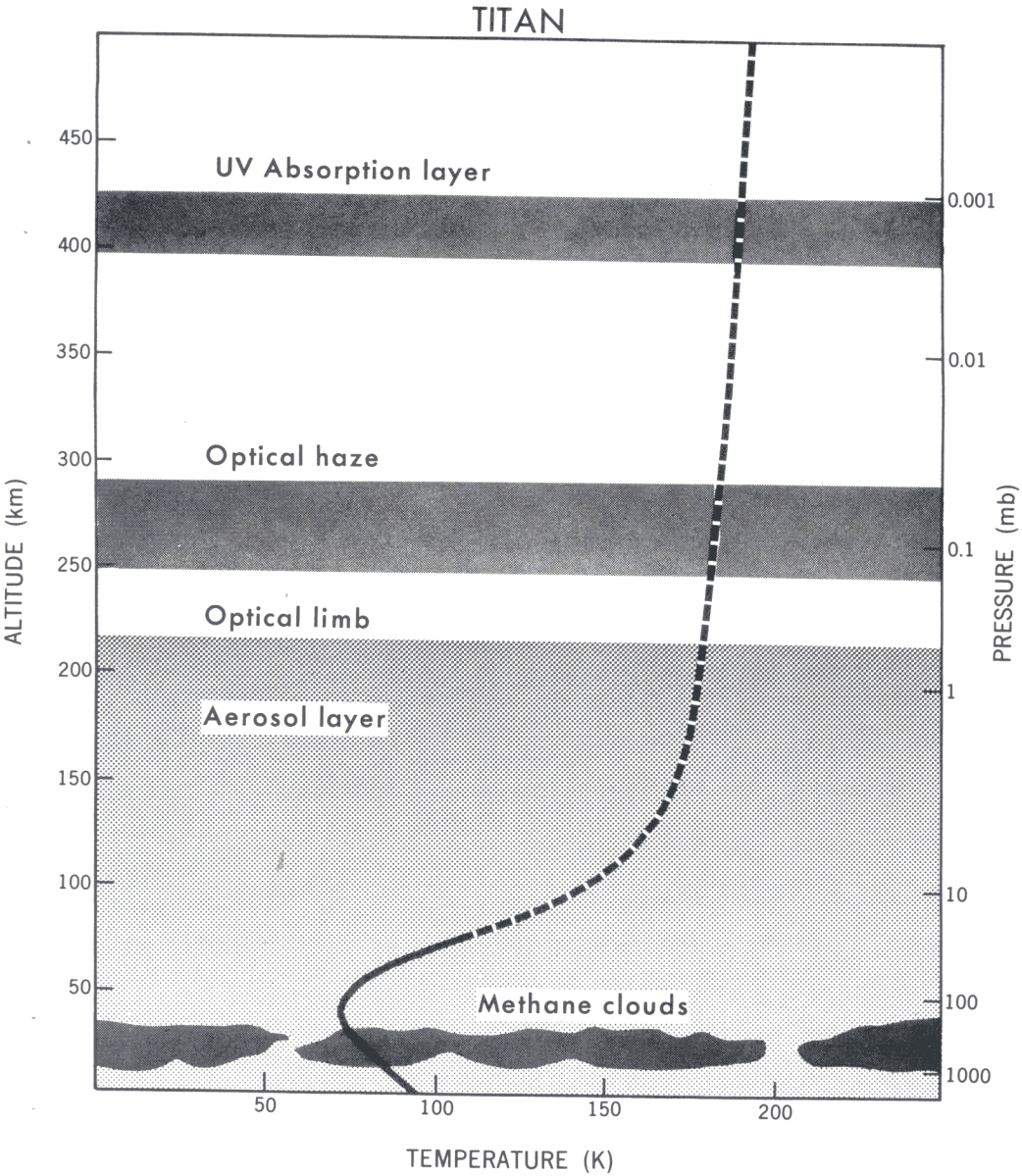

FIG. 4. Vertical profile of temperature and clouds in Titan's atmosphere. [After Hunt and Moore (1982).]

wind estimates. The large stratospheric temperature gradients could produce superrotating cyclostrophic winds of 100 m s^{-1} near the 1-mb level (Flasar *et al.*, 1981a). Titan's circulation should have much in common with the slowly rotating Earth circulation models of Williams and Holloway (1982, Fig. 3; 1985). If so, maximum westerly winds should occur near 75° latitude with jets just below the tropopause and in the stratosphere. The latter could be associated with the observed dark polar collar (Smith *et al.*, 1981). Easterlies could occur in the summer hemisphere toward solstice. Baroclinic instability should be absent, and indeed no longitudinal variations in brightness temperature have been observed. Temperature inversions at the top of the boundary layer (to which the equatorward flow is confined) and low-temperature gradients between the equator and pole occur in both the model and the atmosphere.

3. Numerical Modeling: Planetary Turbulence, Coherence, Circulations

The basic ideas and modeling results mentioned in the Introduction are discussed in greater detail in this section. We begin by reviewing the nature of barotropic β turbulence and its role in the formation of the major Jovian characteristics: the zonality and multiplicity of the jets. Barotropic β turbulence underlies all forms of planetary turbulence as barotropic β waves can occur in any form of atmosphere (semi-infinite, unbounded, etc.). We then describe QG turbulence, noting how and when baroclinic flows behave like forced barotropic flows and the conditions under which it produces Jupiter-like circulations. The origin and existence of coherent features are described using the shallow water (SW) model, the simplest system to incorporate the necessary divergence effects.

The turbulence studies indicate that in mid-latitudes Jupiter is analogous to a more rapidly rotating Earth. To see whether this analog holds in equatorial regions and to see whether any analogs exist with other planets, ECMs have been evaluated for a wide range of parameter values. The ECM solutions also provide a basis for comparative modeling and for circulation theory, and we end with a brief discussion of their character.

3.1. Planetary Turbulence

3.1.1. Barotropic β Turbulence. Barotropic flows behave like two-dimensional (2D) turbulence on the smaller scale, $M \equiv L_\beta^2/L^2 > 1$, where M is the wave steepness factor. Recent studies, while confirming the well-known

tendency of the stream function toward larger scale and the vorticity toward smaller scale, have revealed that interactions are far more intermittent in space and time than originally thought. These result in the formation of coherent, small-scale, high-vorticity regions and enstrophy cascade spectra that range from k^{-3} to k^{-6}, depending on the form of energy input and dissipation (Fornberg, 1977; Basdevant *et al.*, 1981; McWilliams, 1984). Theories based solely on spectral decomposition no longer provide an adequate description of turbulence.

On the larger scale, $M < 1$, barotropic flows display a β-wave dynamics that interacts with the turbulent dynamics only at the transitional scale L_β (Rhines, 1975). At this scale, β-wave dispersion interrupts the expansion of the 2D eddies to retard the energy decascade and to create resonant triads that focus the energy into alternating east–west zonal jets. The anisotropy of the eddies and the zonality of the final flow are mainly due to the anisotropy of the dispersion relation for β waves. At the equator, the nondispersive form of the Kelvin wave relation implies that Kelvin waves cannot be energized by 2D energy decascades even though it also implies that Kelvin waves triads are always resonant and potentially dominant. However, Kelvin waves become dispersive in the presence of shear (Boyd, 1984) so Kelvin turbulence may be possible even though β turbulence normally prevails globally.

The generation of zonal jets is not fully understood. In resonant triads, fully zonal flows cannot gain or lose energy and only act as a catalyst in the exchange between the other two waves (Longuet-Higgins and Gill, 1967; Gill, 1974). However, near-zonal flows can be energized by triad resonances, while near-resonant and sideband interactions can bridge the gap to full zonality (Yamagata and Kono, 1976).

Homogenously forced β turbulence produces alternating jets that are barotropically stable (Rhines, 1975), but inhomogenous forcing produces westerlies — that could become unstable — in the forcing latitudes and easterlies in the unforced regions. The character of locally forced zonal flows can be explained either deterministically using vortex separation ideas based on helicity transfer (Kuo, 1950) or statistically using potential vorticity mixing (Eady, 1954). The latter shows that steady forcing leads to easterlies of magnitude $\bar{u} = -(1/2\beta)\overline{q^2}$, which translates in the Lagrangian view to $\bar{u} = -\frac{1}{2}\beta\overline{y_m^2}$, where $q = \beta y_m$ and y_m is the latitudinal mixing length. For Jupiter, the observed winds of $\bar{u} \sim 20$ m s^{-1} (and $\beta = 4 \times 10^{-9}$ km^{-1} s^{-1}) imply a mixing length of 3000 km, a value consistent with the observed eddy sizes.

The development of anisotropy and zonality from freely evolving homogeneous eddy fields and from forced homogenous and inhomogenous eddy fields has been demonstrated both in laboratory experiments (Whitehead, 1972; de Verdiere, 1980; McEwan *et al.*, 1980) and in numerical studies

with Jovian and terrestrial parameters (Rhines, 1975, 1977; Williams, 1975a,b, 1978; Basdevant *et al.*, 1981; Haidvogel and Rhines, 1983). Eddy forcing is normally based on simple Markovian closure schemes that represent the growth and decay of baroclinic instabilities in midlatitudes and that represent waves created by convection in the tropics.

A solution with Jovian parameters in Fig. 5 reflects the globally homogenous forcing during the early stages. As the energy level increases and energy decascades to larger scales, β-wave propagation sets in, with the steepness of the waves indicating their nonlinear origin. The eddies cease growing as wave propagation takes over. Alternating stable, zonal currents of scale L_β develop from the waves, with the associated waves and currents moving in the same direction, and the system eventually equilibrates. Equatorial jets can be produced by enhanced tropical forcing that is symmetrical about the equator (as are β waves), (Williams, 1978, Fig. 18). Coherent vortices are absent from the flow in Fig. 5 because divergence effects are excluded. Calculations with the more general SW model remedy this deficiency (Williams and Wilson, 1985).

3.1.2. QG Turbulence. Although QG flows possess a 3D vortex stretching mechanism they behave more like 2D flows — when β and boundary effects are negligible — because of analogous potential enstrophy and total energy constraints. Charney (1971) has suggested that QG turbulence could be isotropic if the potential vorticity is defined in terms of the stretched vertical coordinate zN/f and that this results in the available potential and kinetic energies being equipartitioned and having κ^{-3} spectra, where κ is the total wave number. Spectral closure analyses (Herring, 1980) confirm that flows that are initially homogenous become isotropic at the small scales, barotropic at the large scales and baroclinic at the scale of the energy peak L_0. The barotropization is due to the energy decascade toward larger stretched-vertical and horizontal scales.

A serious limitation with the Charney theory is that there is no way of achieving the vertical homogenization of the initial state from more general states (Herring, 1980). This problem arises because the mixing is two-dimensional even though the potential vorticity is three-dimensional.

More realistic and amenable views of QG turbulence have been obtained using the two-level approximation. The equations for QG_2 turbulence can be written in the barotropic, baroclinic forms

$$\nabla^2\tilde{\psi}_t + J(\tilde{\psi}, \nabla^2\tilde{\psi} + f) + J(\hat{\psi}, \nabla^2\hat{\psi}) = 0 \qquad (3.1)$$

$$(\nabla^2 - k_R^2)\hat{\psi}_t + J(\tilde{\psi}, (\nabla^2 - k_R^2)\hat{\psi}) + J(\hat{\psi}, \nabla^2\tilde{\psi} + f) = 0 \qquad (3.2)$$

where k_R is the deformation wave number. These equations immediately reveal the main characteristic of QG_2 flows: baroclinic flows can generate barotropic flow, but barotropic initial states remain barotropic.

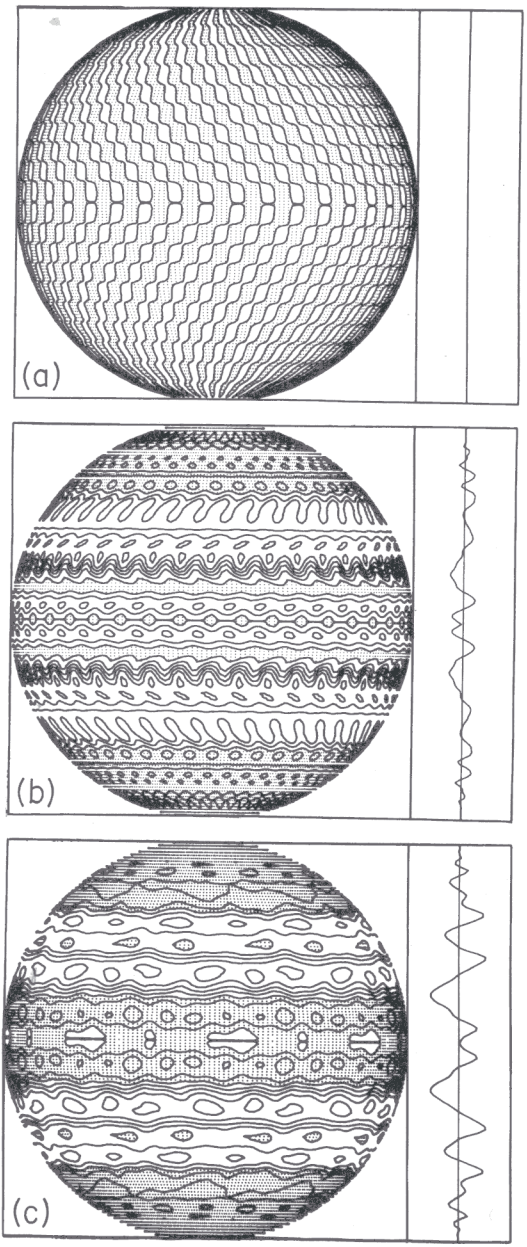

FIG. 5. Formation of multiple zonal currents in a forced barotropic β-turbulence model with Jovian parameters. (a) Day 4.6, (b) day 46, (c) day 161. The flow initially reflects the homogeneous eddy forcing and then develops Rossby waves and finally alternating zonal currents. The contour interval of the stream function, 40 $km^2\ s^{-1}$, is doubled in (c), and negative values are shaded. The zonal wind profile has a scale of ± 100 m s^{-1} and a zero value at the center line. [After Williams (1978). Reproduced with permission from *Journal of the Atmospheric Sciences*, a publication of the American Meteorological Society.]

Analysis of the resonant wave triads of these equations indicate that barotropic primary waves prefer to interact in pure barotropic triads at all scales, whereas baroclinic primary waves prefer to interact in pure baroclinic triads only at small scales and in mixed barotropic–baroclinic triads at large scales (Yamagata, 1976, 1977; Kim, 1978; Jones, 1978; Salmon, 1978, 1980). The barotropic–baroclinic interaction is only really effective at L_R, a scale that provides the valve through which baroclinicity flows into barotropy—but not vice versa. Thus, QG_2 turbulence theory also predicts large-scale barotropy and small-scale isotropy.

How QG_2 flows evolve depends on their initial configuration and on the scale of the energy input relative to L_R and L_β. Rhines (1977, Fig. 19) describes the five basic paths. In general, when the dominant eddy scale L is less than L_R, the two layers are decoupled and each exhibits a separate 2D turbulence; but when $L > L_R$, the layers lock together and behave as a single barotropic layer with the eddies expanding until β-wave effects are felt.

Numerical studies of both freely evolving flows (Rhines, 1975, 1977, 1979) and of equilibrated flows with atmospheric and oceanic forms of forcing and geometry and with idealized (doubly periodic) domains (Steinberg, 1973; Barros and Wiin-Nielsen, 1974; Williams, 1975b, 1979a; Holland, 1978; Holland and Rhines, 1980; Salmon, 1980; Haidvogel and Held, 1980; McWilliams and Chow, 1981) all display the elementary QG_2 turbulent processes described above. The differences between turbulence in heat-driven atmospheric and wind-driven oceanic channels are minor [cf. Williams (1979b) with McWilliams and Chow (1981)]. Ocean basins behave uniquely, however, with eddies acting to limit the wind driven mean flow in the upper layer by producing a downward momentum flux that induces a mean flow in the lower layer (Holland, 1978; Holland and Rhines, 1980).

For Jupiter, QG_2 turbulence models are forced by weak heating functions that crudely represent the latitudinal imbalance of radiative, convective, and internal heating and that produce baroclinicities ranging from 2 to 40 K and instability wavelengths ranging from 2000 to 9000 km. The QG_2 process model is relevant to Jupiter as it represents all forms of baroclinic instability (internal, unbounded, etc.) except the surface type.

Jovian QG_2 flows, Fig. 6, take about 10 years to spin up because of the weak heating rate and go through alternating phases of baroclinic instability and quiescence. The nonlinear cascades and β effects eradicate all traces of the initial Hadley circulation (with its 2 m s^{-1} uniform zonal wind) and generate a series of highly zonal, alternating easterly and westerly jets that are strongly barotropic and whose scale is close to L_β, not L_R. The intermittent baroclinic instabilities eventually pump the jets up to speeds exceeding 100 m s^{-1}.

No organized meridional cells occur in the QG_2 solutions. Similarities

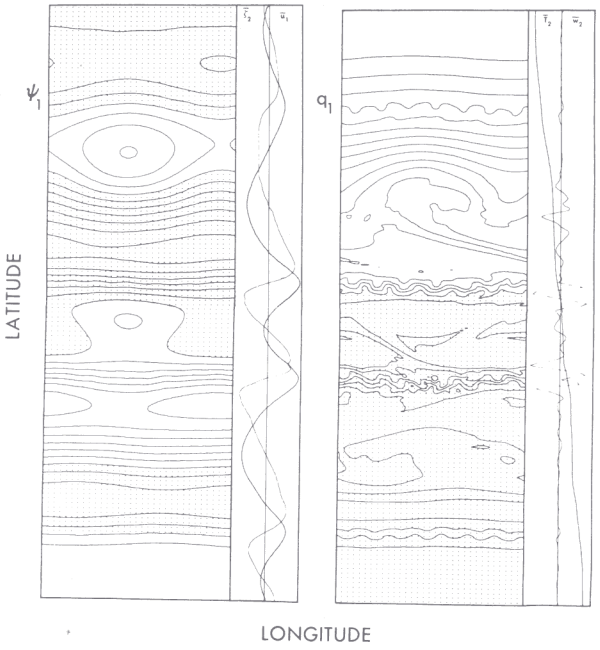

FIG. 6. Formation of multiple zonal currents in a QG_2 turbulence model with Jovian parameters and heating function. The stream function and zonal wind indicate the alternating jets 1773 days into the spinup, while the potential vorticity indicates the scale of the baroclinic instability. The large gyre is a standing neutral baroclinic wave. Negative values are shaded. The zonal wind profile has a scale of ± 160 m s^{-1}. [After Williams (1979a). Reproduced with permission from *Journal of the Atmospheric Sciences*, a publication of the American Meteorological Society.]

between the stream function — rather than temperature or vertical motion — and Jupiter's bands imply that the larger-scale clouds are primarily correlated with horizontal variations in pressure, as befits a quasi-barotropic circulation. Such mechanically induced clouds resemble terrestrial cirrostratus and make the motions remarkably visible.

3.2. Planetary Coherence

3.2.1. Geostrophic Regimes. Most planetary-scale motions are governed by geostrophy, but their characteristics can vary widely depending on their scale relative to the deformation scale L_R. The simplest system capable of describing all the geostrophic regimes (i.e., types of motion) is the shallow-

water (SW) model, whose equations reduce under geostrophy to a single equation for the geopotential height—the general geostrophic equation

$$h_t - \nabla \cdot \left(\frac{h}{f^2} \nabla h_t \right) + \frac{h}{m} h_x (f^{-1})_y - J\left(h, \frac{h}{f^2} \zeta \right) - J\left(\frac{h}{f}, K \right) = 0 \quad (3.3)$$

where $\zeta \equiv \nabla \left((1/f) \nabla h \right)$, $K \equiv (1/2f^2)(\nabla h)^2$, $J(h, \alpha) \equiv m^{-1} (h_x \alpha_y - h_y \alpha_x)$, $(x, y) = a(\lambda, \theta)$, and $m = \cos \theta$ (Williams, 1985). If Eq. (3.3) is nondimensionalized and parametric ordering relationships are chosen, we obtain the planetary geostrophic (PG), intermediate-geostrophic (IG), and the QG sets of subequations that describe motions at the large, intermediate, and synoptic scales. Intermediate motions occur near the scale $L_I = (L_D^2 L_B)^{1/3}$, where $L_D = (gH)^{1/2}/f$ and $L_B = f/\beta$ (Charney and Flierl, 1981). Dispersion (second term) and vorticity advection (fourth term) dominate in the QG regime; nonlinear divergence due to interface displacement (third term) dominates in the PG regime while dispersion and divergence act in balance in the IG regime.

The two types of nonlinearity in the above equation act in different ways. That due to divergence acts at IG scales to preserve correlations and phase information against dispersion, thereby producing such highly predictable phenomena as solitary waves. That due to vorticity advection acts at QG scales as a turbulent scrambler of information. Coherence and turbulence may thus coexist by occurring at widely separated scales.

3.2.2. Coherent Features. Coherent features are essentially of two forms: (1) analytical solitary waves and (2) multivalued modons. Planetary features may be further categorized by dynamical balance, scale, amplitude, symmetry, and location [e.g., Rizzoli (1982)].† The description of modons requires multivalued functions that contain finite discontinuities in the radial vorticity gradient so their physical significance has been questioned. The relevance of a theoretical vortex depends on how readily it can occur, an issue that has only recently been addressed for both analytical forms (Williams and Yamagata, 1984) and multivalued forms (Flierl *et al.*, 1983).

The long-lived, coherent vortices that occur at IG scales are based on solitary Rossby waves travelling westward at close to the long-wave speed $c_\beta = -\beta L_D^2$. In mid-latitudes they coalesce during collisions and are sometimes referred to as Rossby density-vortices (Clarke, 1971) to distinguish them from the Rossby shear-solitons of Long (1964). At the equator, the solitary waves do not coalesce and behave like the Rossby density-soliton of Boyd (1980). The IG balance between dispersion and nonlinear steepening

† Hurricanes differ from most other isolated features in that their strong external energy sources and sinks, rather than their internal inertial balances, hold them together.

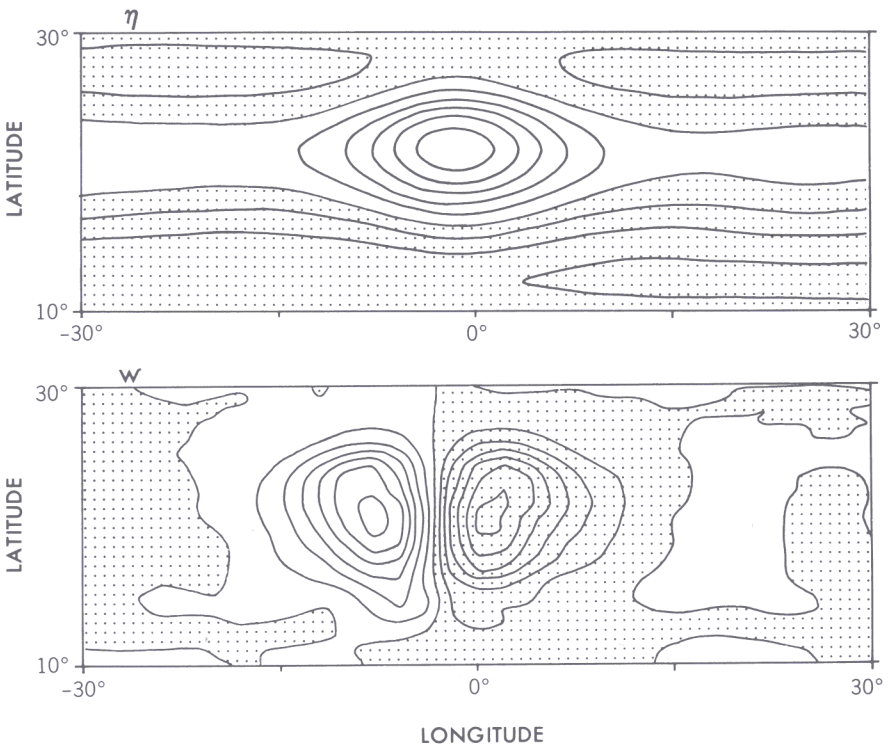

FIG. 7. Closeup of flow near a GRS-like anticyclonic IG vortex located in an anticyclonic shear zone, from the shallow-water model of Williams and Yamagata (1984). Diagram shows height variations and vertical motion after 5 years of evolution. The contour intervals are 1 km and 0.1 cm s^{-1} and negative values are shaded. Computational domain extends over 180° longitude. Such vortices have been maintained in numerical solutions for periods in excess of a century. [After Williams and Yamagata (1984). Reproduced with permission from *Journal of the Atmospheric Sciences,* a publication of the American Meteorological Society.]

due to divergence holds more readily for anticyclonic motion than for cyclonic. However, long-lived coherent cyclones can occur in strong easterly currents (Williams and Yamagata, 1984).

3.2.3. Jovian Vortices. Integrating the SW equations with Jovian parameters shows that vortex behavior varies with latitudinal location and zonal flow environment (Williams and Wilson, 1985). In mid-latitudes (30–60°), IG vortices exist indefinitely but in the subtropics (10–30°) vortex existence is conditional: in the absence of zonal flows they decay in about 1000 days by generating equatorial disturbances, but when Jupiter-like zonal flows are introduced, the vortices can exist indefinitely. A GRS-like vortex has been simulated for 10 years (Fig. 7) and for over 100 years in a less-dissipative

model (Williams and Wilson, 1985). In the tropics (0–10°), Boyd's (1980) solitary β waves occur readily in the SW model and also in the ocean, but apparently not on Jupiter.

Coherent vortices are generated when barotropic instability occurs at the IG scale, whereas periodic disturbances are generated by instability at the QG scale. The number of solitary vortices produced depends on the criticality of the anticyclonic shear zone and on the form of the initial perturbation. Moderately unstable currents produce a small number of well-spaced vortices resembling the Large Ovals (Fig. 8). To produce a *single* permanent vortex, like the GRS, requires a weak instability acting over a long time† in a weakly dissipative atmosphere. This genesis is more convincingly demonstrated in Williams and Wilson (1985) than in Williams and Yamagata (1984). During the development of an instability, perturbations can progress from periodic waves to modulated waves to wave packets to multiple solitary vortices and finally to single solitary vortices.

According to the preceding numerical studies, the uniqueness of the GRS can be attributed to the weakness of the generating instability, the width of the zone, and to the inhomogeneity of the initial perturbation. This is the only theoretical explanation for the uniqueness of the GRS that has been put forward. The modeling also suggests that the 40 to 25° longitudinal shrinkage of the GRS and changes in its drift rate could be due to very small changes in zone width. The vertical motion associated with IG vortices (Fig. 7) provides an observational test of the theory, but the weakness of vertical motions compared to horizontal ones makes detection difficult. To explain the amplitude of the cloud-level winds in the GRS requires models with continuous stratification and with baroclinicity.

3.3. Comparative Global Circulations

3.3.1. Circulation Theory. Although GFD concepts explain many of the regional aspects of planetary circulations, no comprehensive global views have been developed other than the ECM syntheses developed by Smagorinsky *et al.* (1965). Substantial theories have, however, been developed for quasi-geostrophic scale motions in the mid-latitudes of Earth's atmosphere and oceans.

Ocean theories proceed by exploiting the vast difference between the response times of the wind-driven circulations (10 years) and the thermohaline circulations (10^3 years). The wind-driven circulation theories can assume a known stable stratification and can then describe the flow by evaluating the mixing of potential vorticity along density surfaces (Holland *et al.*,

† About 10 years, the time scale for Large Oval development and for zonal flow buildup in circulation models.

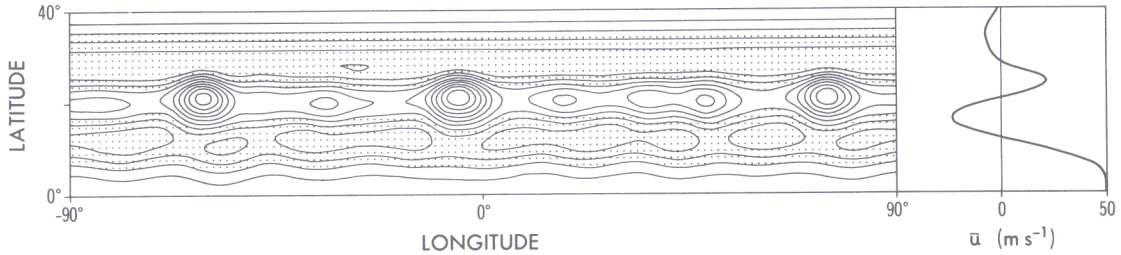

FIG. 8. Multiple isolated, coherent vortices resembling Jupiter's Large Ovals are produced by the weak barotropic instability of an anticyclonic shear zone acting on the IG scale. The height variations and zonal wind profile are produced by a shallow water model with Jovian parameters. The contour interval is 1.5 km and negative values are shaded. [After Williams and Yamagata (1984). Reproduced with permission from *Journal of the Atmospheric Sciences*, a publication of the American Meteorological Society.]

1984). These theories indicate that upper level motions penetrate downward to a depth h_β. Perhaps Jovian dynamical and thermodynamical problems can be similarly segregated.

Atmospheric circulations are turbulent, the fundamental description of which requires that time variations be treated equally with spatial variations. Only the two-point, two-time spectral closure models for velocity variance and Green's function, derived from the direct interaction approximation of Kraichnan† (1959), achieve this fundamental level of description (Kraichnan and Montgomery, 1979; Rose and Sulem, 1978). The spectral closure models for QG_2 turbulence (Salmon, 1978, 1980) indicate the degree of complexity and insight needed to develop a fundamental understanding of atmospheric and oceanic circulations. Simpler parameterizations and climate models avoid the basic dynamical issues.

3.3.2. QG_2 Circulations. The QG_2 model (Phillips, 1956) indicates how mid-latitudinal circulations depend on the basic external parameters f_0, β, and N. For the normal heating rate and surface drag, the circulation changes from an axisymmetric flow at $\Omega^* \leq \frac{1}{4}$, to a wavelike jet at $\Omega^* = \frac{1}{2}$, to an irregular jet at $\Omega^* = 1$, and to double jets at $\Omega^* = 4$, where $\Omega^* = \Omega/\Omega_E$ is the rotation rate relative to the existing value Ω_E (Williams and Holloway, 1985). When drag is removed the double jets coalesce into a stronger and wider jet in keeping with the L_β relation, while the two sets of baroclinic eddies become one without changing scale. This clearly indicates that barotropic processes, not baroclinic ones, determine jet scales. When $\beta = 0$ no jets occur at any value of f_0, only intense irregular eddy motion; this contrasts with annulus circulations where zonal flows always occur because the geometry inhibits nonlinear eddy development. When both β and drag are absent, large gyres occur (Williams, 1979b).

Predictability should be greater on the larger QG scales‡ than on the smaller because of the β blocking effect at L_β—but only if the surface drag is weak and the baroclinic eddies are small, as on Jupiter. For Earth, the surface drag is a major source of flow irregularity on both the turbulent and wave scales (Williams, 1979b), and it is debatable whether predictability on the wave scales is greater (Basdevant *et al.*, 1981) or the same (McWilliams and Chow, 1981) as on the turbulent scales. Flows are more predictable when baroclinic waves fill the domain and thereby limit nonlinear exchanges, as on Mars.

† Kraichnan's creation of the spectral turbulence models ranks as one of the great achievements of modern theoretical physics. It is regretable that its planetary assimilation has been so limited.

‡ Divergence gives motions coherence and predictability on the even larger (IG) scale.

3.3.3. Moist Circulations. When an idealized ECM—with moisture, a swamp surface, and annual mean heating parameters [see Holloway and Manabe (1971) for details]—has its relative rotation rate varied from $\Omega^* = 0$ to 8, its circulations also go from quasi-symmetric to multijet, but they also incorporate a tropical regime. The circulation at $\Omega^* = 4$ is analogous to Jupiter's (Fig. 9) [Williams and Holloway (1982, 1985), see also Hunt (1979)]. These circulations are made up of two types of quasi-geostrophic flow (QG_A, QG_B) and a tropical flow. The QG_A type has an eddy angular momentum transport traversing a diffuse jet in high latitudes, while QG_B has an eddy transport converging on a sharp jet in mid-latitudes (Fig. 9). Nonlinear and linear baroclinic instabilities have similar distinctions (Simmons and Hoskins, 1980). Both types have three meridional cells, two direct and one indirect. The tropical flow has upper-level westerlies and surface easterlies and is due to Hadley cell deflection and to tropical eddy action. The Hadley circulation only extends to about 10° latitude when $\Omega^* = 4$, compared to about 30° when $\Omega^* = 1$, in keeping with the Ω^{-1} relation of Held and Hou (1980). The three forms of jet overlap extensively at $\Omega^* = 1$ to give Earth a most complex meteorology.

Below $\Omega^* = \frac{1}{4}$ baroclinic instability is absent, surface torques are weaker by a factor of 10 and the easterly trade winds vanish. Comparing flows with rotation rates above and below $\Omega^* = \frac{1}{4}$ makes it apparent that waves propagating from the baroclinic eddies create the easterlies in the tropics, as in β turbulence. At the transitional value of $\Omega^* = \frac{1}{4}$, baroclinic instability is shallow and only occurs in the lower troposphere, in keeping with the decline in penetration depth, $h = f^2 u_z/\beta N^2$, as Ω decreases (Held, 1978).

3.3.4. Dry Circulations. If moisture dynamics is excluded from the ECM, the tropical form of circulation does not materialize and the meridional and zonal flows are much weaker near the equator, at all Ω^* values. The tropical cell is just the secondary direct circulation associated with the Ferrel cell of the mid-latitudinal jet. Strong motions only occur in the tropics if the heating is enhanced there, either by moisture or by internal heating. If surface drag is omitted, only easterly winds occur in the tropics (Williams and Holloway, 1985).

3.3.5. Moist Axisymmetric Circulations. Natural Hadley circulations occur when $\Omega^* < \frac{1}{4}$ but they are not axisymmetric—except when time averaged—as longitudinally varying convective and dissipative eddies remain. To estimate the role of baroclinic instability at $\Omega^* = 1$, attempts have been made to define an "ideal" or axisymmetric Hadley circulation in which all longitudinal variations are artificially suppressed. Unfortunately, this

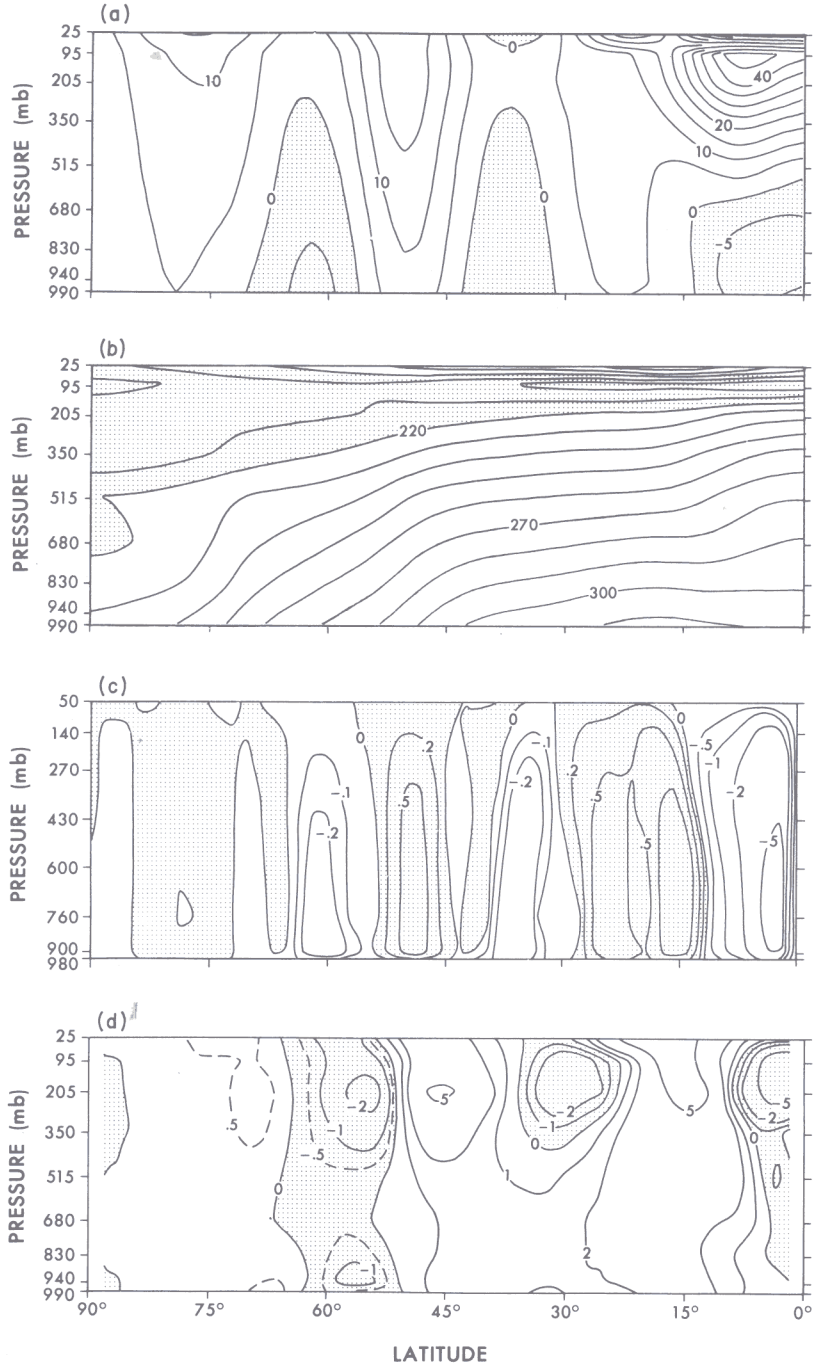

FIG. 9. The time and longitudinally averaged fields of the circulation of an idealized Earth-like model atmosphere when the rotation rate is 4 times the normal value, i.e., $\Omega^* = 4$. Diagram shows zonal motion (a), temperature (b), meridional stream function (c), and northward eddy angular momentum transport (d), with units of $m\,s^{-1}$, K, $10^{13}\,g\,s^{-1}$, $10^7\,m^3\,s^{-2}$, respectively. The three basic types of circulation occur: the tropical up to 10° latitude and types QG_B, QG_A at 50°, 80°. [After Williams and Holloway (1982, 1985).]

action also eliminates the natural dissipation and dispersion mechanisms that must then be replaced by ambiguous vertical mixing representations. Axisymmetric circulations are crucially dependent on these dissipation schemes and thus appear to be of marginal physical significance, although they remain of great historical interest.

A better way of gauging the role of the eddies—other than by altering Ω^*—is by reducing their size and strength artificially by using small global sectors. "Small-eddy" circulations can be made to approach the ideal Hadley circulation gradually while retaining natural dissipation and mixing.

Moist axisymmetric ECM flows are dominated by subgrid transports (convection, dissipation) so their meridional circulations lack simplicity and uniqueness (Williams and Holloway, 1985). At the lower rotation rates ($\Omega^* \leq 1$) the zonal flow consists of a single broad westerly jet while at higher rotation rates it consists of two westerly jets, one in the tropics and one in mid-latitudes. The tropical jet has the same width and amplitude as in the natural system but the mid-latitude jet is broader and stronger (60 m s^{-1} compared to 15 m s^{-1}).

If the axisymmetric westerlies are stronger than the natural westerlies, is it correct to conclude that eddies reduce the zonal momentum in mid-latitudes [cf. Schneider and Lindzen (1977)]? The answer is no, on two counts. First, the axisymmetric winds are stronger because the axisymmetric thermal gradients are stronger. Second, the time required to create the axisymmetric flow is much longer than the time required by the eddies to create the natural jets. Thus, the natural state does not sense the axisymmetric state, just as synoptic states do not sense the seasonal cycle.

3.3.6. Diurnal Circulations. As the rotation rate drops below the transitional value of $\Omega^* = \frac{1}{4}$, the kinetic energy of the ECM continues to increase and the axis of the Hadley jet moves poleward until a limit is reached near 75° latitude (Williams and Holloway, 1982). Kinetic energy peaks at $\Omega^* = \frac{1}{8}$ and then decreases as cyclostrophy takes over from geostrophy.

A second transition occurs at $\Omega^* = \frac{1}{16}$ when diurnal heating variations become important. The equatorward transport of angular momentum and heat by the diurnal eddies changes the narrow polar jets of the nondiurnal state into broad global superrotating currents resembling those of Venus. Below $\Omega^* = \frac{1}{64}$, the diurnal variations dominate rather than modify the circulations and produce subsolar to antisolar flows.

3.3.7. Oblique (Seasonal) Circulations. Seasonal variations illustrate most simply the sensitivity of ECM behavior to thermodynamical forcing. Varying the planetary obliquity θ_p up to 90° latitude gives the full range of response. Without ocean heat storage, temperature maxima occur in mid-

latitudes when $\theta_p = 10°$ and at the pole when $\theta_p \geq 20°$ — a typical planetary value (Table I).

Zonal flows are generally easterly in the summer hemisphere and westerly in the winter hemisphere as a result of these temperature gradients (Williams and Holloway, 1982, 1985; Hunt, 1982). The easterlies are produced by Hadley circulations, which straddle the equator symmetrically from $\pm 30°$ when $\Omega^* = \frac{1}{2}$ to $\pm 15°$ when $\Omega^* = 4$ for most θ_p values. Only in an extreme case ($\Omega^* = \frac{1}{2}$, $\theta_p = 90°$) does the cell extend from pole to pole and do unique diagonal convective bands occur in the summer tropics. Normally eddies are most active in the winter hemisphere.

Hadley circulations cool the summer hemisphere and heat the winter tropics, which is then cooled by eddies transferring heat to the winter pole. Angular momentum balance is achieved globally with the meridional circulation providing the exchange between the positive surface torque in the winter hemisphere and the negative torque in the summer hemisphere.

3.3.8. Planetary Implications. The ECM solutions suggest that when a simplified, Earth-like atmosphere is placed in the rotational configuration of another planet it displays that planet's form of motion despite thermodynamical and other differences. Table I contains a preliminary classification of planetary circulations by rotation rate and obliquity.

For Earth, the solutions indicate that the poleward eddy momentum transport is a consequence of the hybrid mix of three circulation types. Mars has a strong seasonal variation because it lacks oceanic thermal inertia and so its circulation resembles those of our simple ECM at $\Omega^* = 1$ (Williams and Holloway, 1982, Fig. 2c). Venus appears to lie in the narrow range of Ω values where diurnal effects modify rather than dominate the circulation.

Both Jupiter and the moist ECM at $\Omega^* = 4$ have pre-eminent tropical jets and multiple, highly zonal, extratropical jets, plus assorted eddies [cf. Williams and Holloway (1982, Fig. 4)]. If the analog is completely valid, Jupiter should have easterly trade winds in the lower tropics. However, the analog is weakest in the tropics because it is uncertain whether moisture and surface stress occur on Jupiter or whether enhanced internal heating and cumulus friction can act in an equivalent way. Tropical westerly jets can be produced either by Hadley circulations or by enhanced eddy activity in β-turbulence cascades. Further studies are needed to determine which process, if either, occurs.

Saturn, Uranus, and Neptune should resemble Jupiter at equinox but during solstice their summer hemispheres should contain easterly winds. Internal heating could reduce seasonal variations on Saturn and Neptune. On Uranus, diagonal convective bands could occur in the summer tropics

while a Hadley cell straddles the equator to about $\pm 20°$ latitude — unless the rotational influence is unexpectedly weak, in which case it could go from pole to pole.

4. Planetary Prospects

4.1. Observations

The upcoming Voyager encounters with Uranus (in 1986) and Neptune (in 1989) will complete the recent *reconnaissance* of the solar system by some two dozen spacecraft (Kondratyev and Hunt, 1982; Beatty *et al.*, 1981) and reveal whether or not these planets fit into the general scheme. Although planetary *exploration* appears to be no more than a remote possibility at this time, detailed monitoring of Jupiter is imminent.

The long period, high-resolution observation of Jupiter by the Galileo orbiter and by the Space Telescope should yield details of wave and eddy interactions that, if imaginatively analyzed, could reveal the vertical structure of the atmosphere. For example, baroclinic instabilities have speeds and growth rates that vary as u_z and u_z/N, so the shear and stability could be estimated from temporal data. Instabilities may also be absolute or advective and exhibit spatial or temporal growth depending on the ratio of $\hat{u}/\tilde{u}$ (Farrell, 1982, 1983). In absolute (advective) instabilities the front and rear edges of a pulse move in opposite (identical) directions. Thus the study of wave packet evolution could also give a value for the vertical shear.

The Galileo probe of Jupiter's equatorial atmosphere should test for moisture, vertical motion, and vertical shear to determine whether a Hadley circulation exists. Deeper probes are needed to explore the lower atmosphere, while multiple mid-latitudinal probes are needed to measure baroclinicity.

4.2. Modeling

The completion of the class of circulations generated by the ECM for a semi-infinite atmosphere requires the evaluation of models for vertically unbounded fluids. Such models should also reveal how baroclinic instabilities, Hadley circulations, etc., behave in the absence of a surface. Evaluating ocean models as a function of Ω^* would supplement and guide such calculations.

The existence of Rossby vortices and solitons in models with a continuous stratification needs to be studied to help circumscribe the vertical form of the

atmosphere. Then JCMs can be designed to synthesize the results from the different models for the different phenomena. Our understanding of Jupiter's, jets, vortices, and eddies is good at the basic level and should be greatly enhanced in this decade.

4.3. Theory

To deepen our understanding of the various circulations requires that some basic GFD problems concerning geostrophic regimes, waves, instabilities, and turbulence be resolved (see CD85). Perhaps the most important immediate problem is to determine the influence of nonlinear divergence on the energy decascade into zonal flow at the IG scales and at the equator.

To improve numerical models, we need to discover which methods best describe the intermittent, part random, part coherent nature of the 2D exchanges that underlie much of planetary turbulence and must be allowed for in subgrid closure schemes. Can renormalized perturbation schemes be created for the planetary subgrid scales? Can fractal dimensions really describe the space occupied by dissipative eddies and explain intermittency (Rose and Sulem, 1978)? Or can the successive averaging methods of renormalized group theory be used to design layers of subgrid scales to give better eddy representations (Rose, 1977)? The original nonlinear viscosity designed for planetary modeling (Smagorinsky, 1963) appears to have "succeeded brilliantly" (Leslie, 1982) for 3D turbulence—more so, perhaps, than for quasi-2D motions. Perhaps direct simulations with resolutions greater than the 256^3 and 256^2 modes used for quasi-3D turbulence (Brachet *et al.*, 1983) and 2D turbulence (Frisch and Sulem, 1984) will answer some of these questions.

5. Conclusion

Fool: "The reason why the seven stars are no more than seven is a pretty reason."
Lear: "Because they are not eight."
Fool: "Yes indeed. Thou woulds't make a good fool."

W. Shakespeare

In this article we have tried to indicate how meteorological unity might exist among the planets of the solar system and how it can be used to construct preliminary or provisional models for individual planets. The

reason the unity exists is because no disunity is apparent. Whether this attempt to recreate the solar system in Earth's image has any more merit than previous views only time, observation, and better theory will decide. For now, its advantage appears to be that it yields explanations—where none existed before—of various phenomena without apparent inconsistencies and with verifiable (or falsifiable) predictions.

For Jupiter, the main implication of the GFD view is that the zonally banded form of circulation, with its multiple easterly and westerly jets, is essentially a characteristic of quasi-horizontal turbulence on a rapidly rotating sphere. The flow is energized by small-scale (L_R) baroclinically unstable eddies that cascade energy toward the large scale (L_β), where they generate the Rossby waves that evolve into zonal currents. These jets can become barotropically unstable and produce solitary waves resembling the Great Red Spot and Large Ovals. The greatest uncertainties at present concern the extent to which eddy action or Hadley cell deflection produce the tropical jet and the extent to which baroclinicity influences the GRS.

In the past decade, modeling and observation have drastically altered our perspective of Earth and our view of the solar system. There are indeed connections between the terrestrial and planetary meteorologies, but these are often subtle and involve great parametric changes. The planets are no longer semimythical bodies, glimpsed "through a glass, darkly" by inadequate telescopes or ideas, but real worlds demanding imaginative interpretation.

Acknowledgments

My planetary studies have been greatly influenced by the ideas and philosophy of Joseph Smagorinsky, from the time he gave the 1963 Symons memorial lecture as meteorological spokesman for the New Frontier to his present role as senior meteorological statesman. His credo of parametric, computational, and cultural freedom and his belief that meteorologists could contribute to the exploration of space have been a constant source of encouragement and enlightenment.

This paper would never have materialized without Syukuro Manabe, who persuaded me that reviewing the unknown was possible and who accepted that it took longer. I am also grateful to Leith Holloway and John Wilson for collaboration in developing many of the ideas in this paper, to Joan Pege for typing, to Phil Tunison for drafting, and to Sanjay Limaye for preparing Fig. 3.

References

Allison, M., and Stone, P. H. (1983). Saturn meteorology: A diagnostic assessment of thin-layer configurations for the zonal flow. *Icarus* **54,** 296–308.

Antipov, S. V., Nezlin, M. Y., Snezhkin, E. N., and Trubnikov, A. S. (1982). Rossby soliton in the laboratory. *JETP* **82,** 145–160 [in Russian].

Barros, V. R., and Wiin-Nielsen, A. (1974). On quasi-geostrophic turbulence: A numerical experiment. *J. Atmos. Sci.* **31,** 609—621.

Basdevant, C., Legras, B., Sadourny, R., and Beland, M. (1981). A study of barotropic model flows: Intermittency, waves and predictability. *J. Atmos. Sci.* **38,** 2305–2326.

Beaumont, D. N. (1980). Solitary waves on an unsymmetrical shear flow with applications to Jupiter's Great Red Spot. *Icarus* **41,** 400–408.

Beatty, J. K., O'Leary, B., and Chaikin, A. (1981). "The New Solar System." Sky Publishing, Cambridge, Massachusetts.

Beebe, R. F., Ingersoll, A. P., Hunt, G. E., Mitchell, J. L., and Müller, J. P. (1980). Measurements of wind vectors, eddy momentum transports, and energy conversions in Jupiter's atmosphere from Voyager 1 images. *Geophys. Res. Lett.* **7,** 1–4.

Bolin, B. (1956). An improved barotropic model and some aspects of using the balance equation for three-dimensional flow. *Tellus* **8,** 61–75.

Boyd, J. P. (1980). Equatorial solitary waves. Part 1: Rossby solitons. *J. Phys. Oceanogr.* **10,** 1699–1717.

Boyd, J. P. (1984). Equatorial solitary waves. Part 4: Kelvin solitons in a shear flow. *Dyn. Atmos. Oceans* **8,** 173–184.

Brachet, M. E., Meiron, D. I., Orszag, S. A., Nickel, B. G., Morf, R. H., and Frisch, U. (1983). Small-scale structure of the Taylor-Green vortex. *J. Fluid Mech.* **130,** 411–452.

Branscome, L. E. (1982). Jovian dynamics and cloud features. Unpublished manuscript, Department of Meteorology, MIT, Cambridge, Massachusetts.

Brown, J. A. (1969). A numerical investigation of hydrodynamic instability and energy conversions in a quasi-geostrophic atmosphere: Part 1. *J. Atmos. Sci.* **26,** 352–365.

Busse, F. H. (1983). A model of mean zonal flows in the major planets. *Geophys. Astrophys. Fluid Dyn.* **23,** 153–174.

Charney, J. G. (1971). Geostrophic turbulence. *J. Atmos. Sci.* **28,** 1087–1095.

Charney, J. G., and Flierl, G. R. (1981). Oceanic analogues of large scale atmospheric motions. *In* "Evolution of Physical Oceanography" (B. A. Warren and C. Wunsch, eds.), pp. 504–548. MIT Press, Cambridge, Massachusetts.

Clarke, R. A. (1971). Solitary and cnoidal planetary waves. *Geophys. Fluid Dyn.* **2,** 343–354.

Conrath, B. J., and Pirraglia, J. A. (1983). Thermal structure of Saturn from Voyager infrared measurements: Implications for atmospheric dynamics. *Icarus* **53,** 286–292.

Conrath, B. J., and Gierasch, P. J. (1984). Global variation of the para hydrogen fraction in Jupiter's atmosphere and implications for dynamics on the outer planets. *Icarus* **57,** 184–204.

De Verdiere, A. C. (1980). Quasi-geostrophic turbulence in a rotating homogeneous fluid. *Geophys. Astrophys. Fluid Dyn.* **15,** 213–251.

Dickinson, R. E. (1973). Baroclinic instability of an unbounded zonal shear flow in a compressible atmosphere. *J. Atmos. Sci.* **30,** 1520–1527.

Eady, E. T. (1954). The maintenance of the mean zonal surface currents. *Proc. Toronto Met. Conf., 1953,* pp. 124–128. Roy. Met. Soc., London.

Farrell, B. F. (1982). Pulse asymptotics of the Charney baroclinic instability problem. *J. Atmos. Sci.* **39,** 507–517.

Farrell, B. F. (1983). Pulse asymptotics of three dimensional baroclinic waves. *J. Atmos. Sci.* **40,** 2202–2210.

Flasar, F. M., Samuelson, R. E., and Conrath, B. J. (1981a). Titan's atmosphere: Temperature and dynamics. *Nature (London)* **292,** 693–698.

Flasar, F. M., Conrath, B. J., Pirraglia, J. A., Clark, P. C., French, R. G., and Gierasch, P. J. (1981b). Thermal structure and dynamics of the Jovian atmosphere. 1. The Great Red Spot. *JGR, J. Geophys. Res.* **86,** 8759–8767.

Flierl, G. R., Stern, M. E., and Whitehead, J. B. (1983). The physical significance of modons: Laboratory experiments and general integral constraints. *Dyn. Atmos. Oceans* **7,** 233–263.

Fornberg, B. (1977). A numerical study of 2-D turbulence. *J. Comp. Phys.* **25,** 1–31.

Frisch, U., and Sulem, P. L. (1984). Numerical simulation of the inverse cascade in two-dimensional turbulence. *Phys. Fluids* **27,** 1921–1923.

Gall, R. L. (1976). A comparison of linear baroclinic instability theory with the eddy statistics of a general circulation model. *J. Atmos. Sci.* **33,** 349–373.

Gehrels, T. (1976). The results of the imaging photopolarimeter on Pioneers 10 and 11. *In* "Jupiter" (T. Gehrels, ed.), pp. 531–563. Univ. of Arizona Press, Tucson, Arizona.

Gill, A. E. (1974). The stability of planetary waves on an infinite beta-plane. *Geophys. Fluid. Dyn.* **6,** 29–47.

Golitsyn, G. S. (1970). A similarity approach to the general circulation of planetary atmospheres. *Icarus* **13,** 1–24.

Golitsyn, G. S. (1979). Atmospheric dynamics on the outer planets and some of their satellites. *Icarus* **38,** 333–341.

Grey, W. M. (1978). Hurricanes: Their formation, structure and likely role in the tropical circulation. *In* "Meteorology over the Tropical Oceans" (D. B. Shaw, ed.), pp. 155–218. Roy. Met. Soc., London.

Haidvogel, D. B., and Held, I. M. (1980). Homogeneous quasi-geostrophic turbulence driven by a uniform temperature gradient. *J. Atmos. Sci.* **37,** 2644–2660.

Haidvogel, D. B., and Rhines, P. B. (1983). Waves and circulation driven by oscillatory winds in an idealized ocean basin. *Geophys. Astrophys. Fluid Dyn.* **25,** 1–63.

Hanel, R. A., Conrath, B. J., and 11 co-authors (1979). Infrared observations of the Jovian system from Voyager 1. *Science* **204,** 972–976.

Hanel, R. A., Conrath, B. J., Kunde, V. G., Pearl, J. C., and Pirraglia, J. A. (1983). Albedo, internal heat flux, and energy balance of Saturn. *Icarus* **53,** 262–285.

Hatzes, A., Wenkert, D. D., Ingersoll, A. P., and Danielson, G. E. (1981). Oscillations and velocity structure of a long-lived cyclone spot. *JGR, J. Geophys. Res.* **86,** 8745–8749.

Held, I. M., (1978). The vertical scale of an unstable baroclinic wave and its importance for eddy heat flux parameterizations. *J. Atmos. Sci.* **351,** 572–576.

Held, I. M., and Hou, A. Y. (1980). Nonlinear axially symmetric circulations in a nearly inviscid atmosphere. *J. Atmos. Sci.* **37,** 515–533.

Herring, J. R. (1980). Statistical theory of quasi-geostrophic turbulence. *J. Atmos. Sci.* **37,** 969–977.

Holland, W. R. (1978). The role of mesoscale eddies in the general circulation of the ocean: Numerical experiments using a wind-driven quasi-geostrophic model. *J. Phys. Oceanogr.* **8,** 363–392.

Holland, W. R., and Haidvogel, D. B. (1980). A parameter study of the mixed instability of idealized ocean currents. *Dyn. Atmos. Oceans* **4,** 185–215.

Holland, W. R., and Rhines, P. B. (1980). An example of eddy-induced ocean circulation *J. Phys. Oceanogr.* **10,** 1010–1031.

Holland, W. R., Keffer, T., and Rhines, P. B. (1984). Dynamics of the oceanic general circulation: The potential vorticity field. *Nature (London)* **308,** 698–705.

Holloway, J. L., and Manabe, S. (1971). Simulation of climate by a global general circulation model. *Mon. Weather Rev.* **99,** 335–370.

Holton, J. R. (1974). On the trapping of unstable baroclinic waves. *J. Atmos. Sci.* **31,** 2220–2222.

Holton, J. R. (1975). "The Dynamic Meteorology of the Stratosphere and Mesosphere." Meteorol. Monogr. 37, Am. Met. Soc., Boston, Massachusetts.

Houghton, J. T. (1977). "The Physics of Atmospheres." Cambridge Univ. Press, Cambridge.
Hunt, B. G. (1979). The influence of the Earth's rotation rate on the general circulation of the atmosphere. *J. Atmos. Sci.* **36,** 1392–1408.
Hunt, B. G. (1982). The impact of large variations of the Earth's obliquity on the climate. *J. Met. Soc. Japan* **60,** 309–318.
Hunt, G. E. (1983). The atmospheres of the outer planets. *Annu. Rev. Earth Planet. Sci.* **11,** 415–459.
Hunt, G. E., and Müller, J.-P. (1979). Voyager observations of small scale waves in the equatorial region of the Jovian atmosphere. *Nature (London)* **280,** 778–780.
Hunt, G. E., and Moore, P. (1982). "Saturn." Roy. Astron. Soc. and Rand-McNally, London.
Hunt, G. E., Conrath, B. J., and Pirraglia, J. A. (1981). Visible and infrared observations of Jovian plumes during the Voyager encounter. *JGR, J. Geophys. Res.* **86,** 8777–8781.
Hunt, G. E., Müller, J.-P., and Gee, P. (1982). Convective growth rates of equatorial features in the Jovian atmosphere. *Nature (London)* **295,** 491–494.
Iavorskaya, I. M., and Belyaef, Yu. N. (1983). Convective motions in rotating fluid layers. *Advances in Science and Technology of VINITI, Mechanics of Fluids and Gases* **17,** 2–85 [in Russian].
Ingersoll, A. P., and Pollard, D. (1982). Motion in the interiors and atmospheres of Jupiter and Saturn: Scale analysis, anelastic equations, barotropic stability criterion. *Icarus* **52,** 62–80.
Ingersoll, A. P. *et al.* (1979). Zonal velocity and texture in the jovian atmosphere inferred from Voyager images. *Nature (London)* **280,** 773–775.
Ingersoll, A. P., Beebe, R. F., Mitchell, J. L., Garneau, G. W., Yagi, G. M., and Müller, J.-P. (1981). Interaction of eddies and zonal mean flow on Jupiter as inferred from Voyager 1 and 2 images. *JGR, J. Geophys. Res.* **86,** 8733–8743.
Jones, S. (1978). Interactions and instabilities of barotropic and baroclinic Rossby waves in a rotating, two layer fluid. *Geophys. Astrophys. Fluid Dyn.* **11,** 49–60.
Kim, K. (1978). Instability of baroclinic Rossby waves: energetics in a two-layer ocean. *Deep-Sea Res.* **25,** 795–814.
Kondratyev, K. Y., and Hunt, G. E. (1982). "Weather and Climate on Planets." Pergamon Press, Oxford.
Kraichnan, R. H. (1959). The structure of isotropic turbulence at very high Reynolds numbers. *J. Fluid Mech.* **5,** 497–543.
Kraichnan, R. H., and Montgomery, D. (1979). Two-dimensional turbulence. *Rep. Prog. Phys.* **43,** 547–619.
Kuo, H.-L. (1950). The motion of atmospheric vortices and the general circulation. *J. Meteor.* **7,** 247–258.
Leovy, C. B. (1979). Martian Meteorology. *Annu. Rev. Astron. Astrophys.* **17,** 387–413.
Leslie, D. C. (1982). Simulation methods for turbulent flows. *In* "Numerical Methods for Fluid Dynamics" (K. W. Morton and M. J. Baines, eds.), pp. 63–80. Academic Press, New York.
Limaye, S. S. (1985). New estimates of the mean zonal flow on Jupiter. *Icarus* (in press).
Limaye, S. S., Revercomb, H. E., and 6 co-authors. (1982). Jovian winds from Voyager 2. Part 1: Zonal mean circulation. *J. Atmos. Sci.* **39,** 1413–1432.
Lindal, G. F. *et al.* (1981). The atmosphere of Jupiter: An analysis of the Voyager radio occultation measurements. *JGR, J. Geophys. Res.* **86,** 8721–8727.
Lindal, G. F., Wood, G. E., Hotz, H. B., Sweetnam, D. N., Eshleman, V. R., and Tyler, G. L. (1983). The atmosphere of Titan: An analysis of the Voyager 1 radio occultation measurements. *Icarus* **53,** 348–363.
Lindzen, R. S., Farrell, B., Tung, K.-K. (1980). The concept of wave overreflection and its application to baroclinic instability. *J. Atmos. Sci.* **37,** 44–63.
Lipps, F. B. (1963). Stability of jets in a divergent barotropic fluid. *J. Atmos. Sci.* **20,** 120–129.
Long, R. R. (1964). Solitary waves in the westerlies. *J. Atmos. Sci.* **21,** 197–200.

Longuet-Higgins, M. S., and Gill, A. E. (1967). Resonant interactions between planetary waves. *Proc. Roy. Soc.* **A299,** 120–140.

Lorenz, E. N. (1953). The vertical extent of Jupiter's atmosphere. *In* "The Study of Planetary Atmospheres" (E. C. Slipher, ed.), pp. 136–145. Lowell Observatory Rep. AF19(122)-162, Flagstaff, Arizona.

Mahlman, J. D., and Moxim, W. J. (1978). Tracer simulation using a global general circulation model: Results from a midlatitude instantaneous source experiment. *J. Atmos. Sci.* **35,** 1340–1374.

Maxworthy, T., and Redekopp, L. G. (1976). A solitary wave theory of the Great Red Spot and other observed features of the Jovian atmosphere. *Icarus* **29,** 261–271.

McEwan, A. D., Thompson, R., and Plumb, R. A. (1980). Mean flows driven by weak eddies in rotating systems. *J. Fluid Mech.* **99,** 655–672.

McIntyre, M. E. (1972). Baroclinic instability of an idealized model of the polar night jet. *Quart. J. Roy. Meteor. Soc.* **98,** 165–174.

McWilliams, J. C. (1984). The emergence of isolated coherent vortices in turbulent flow. *J. Fluid Mech.* **146,** 21–43.

McWilliams, J. C., and Chow, J. H. S. (1981). Equilibrium geostrophic turbulence 1: A reference solution in a β-plane channel. *J. Phys. Oceanogr.* **11,** 921–949.

Mitchell, J. L. (1982). "The Nature of Large-Scale Turbulence in the Jovian Atmosphere." NASA/JPL Publication 82–34, Pasadena, California.

Mitchell, J. L. *et al.* (1979). Jovian cloud structure and velocity fields. *Nature (London)* **280,** 776–778.

Mitchell, J. L., Beebe, R. F., Ingersoll, A. P., and Garneau, G. W. (1981). Flow fields within Jupiter's Great Red Spot and White Oval BC. *JGR, J. Geophys. Res.* **86,** 8751–8757.

Owen, T., and Terrile, R. J. (1981). Colors on Jupiter. *JGR, J. Geophys. Res.* **86,** 8797–8814.

Pedlosky, J. (1979). "Geophysical Fluid Dynamics." Springer-Verlag, New York.

Pfister, L. (1979). A theoretical study of three-dimensional barotropic instability with applications to the upper stratosphere. *J. Atmos. Sci.* **36,** 908–920.

Philander, S. G. H., and Pacanowski, R. C. (1980). The generation of equatorial currents. *JGR, J. Geophys. Res.* **85,** 1123–1136.

Phillips, N. A. (1954). Energy transformations and meridional circulations associated with simple baroclinic waves in a two-level, quasi-geostrophic model. *Tellus* **6,** 273–286.

Phillips, N. A. (1956). The general circulation of the atmosphere: A numerical experiment. *Quart. J. Roy. Met. Soc.* **82,** 123–164.

Pirraglia, J. A., Conrath, B. J., Allison, M. D., and Gierasch, P. J. (1981). Thermal structure and dynamics of Saturn and Jupiter. *Nature (London)* **292,** 677–679.

Pollack, J. B., and Yung, Y. L. (1980). Origin and evolution of planetary atmospheres. *Annu. Rev. Earth Planet Sci.* **8,** 425–487.

Rhines, P. B. (1975). Waves and turbulence on a beta plane. *J. Fluid Mech.* **69,** 417–443.

Rhines, P. B. (1977). The dynamics of unsteady currents. *In* "The Sea," Vol. 6 (I. N. McCane, J. J. O'Brien, and J. M. Steele, eds.), pp. 189–318. Wiley, New York.

Rhines, P. B. (1979). Geostrophic Turbulence. *Annu. Rev. Fluid Mech.* **11,** 401–441.

Rizzoli, P. M. (1982). Planetary solitary waves in geophysical flows. *Adv. Geophys.* **24,** 147–224.

Rose, H. A. (1977). Eddy diffusivity, eddy noise and subgridscale modelling. *J. Fluid Mech.* **81,** 719–734.

Rose, H. A., and Sulem, P. L. (1978). Fully developed turbulence and statistical mechanics. *J. de Phys.* **39,** 441–484.

Rossow, W. B. (1983). A general circulation model of a Venus-like atmosphere. *J. Atmos. Sci.* **40,** 273–302.

Salmon, R. (1978). Two-layer quasi-geostrophic turbulence in a simple special case. *Geophys. Astrophys. Fluid Dyn.* **10,** 25–52.

Salmon, R. (1980). Baroclinic instability and geostrophic turbulence. *Geophys. Astrophys. Fluid Dyn.* **15,** 167–211.

Samuelson, R. E., Hanel, R. A., Kunde, V. G., and Maguire, W. C. (1981). Mean molecular weight and hydrogen abundance of Titan's atmosphere. *Nature (London)* **292,** 688–693.

Samuelson, R. E., Maguire, W. C., and 5 co-authors (1983). CO_2 on Titan. *JGR, J. Geophys. Res.* **88,** 8709–8715.

Sanchez-Lavega, A. (1982). Motions in Saturn's atmosphere: Observations before Voyager encounters. *Icarus* **49,** 1–16.

Schneider, E. K., and Lindzen, R. S. (1977). Axially symmetric steady-state models of the basic state for instability and climate studies. Part 1: Linearized calculations. *J. Atmos. Sci.* **34,** 263–279.

Schoeberl, M. R., and Strobel, D. F. (1978). The zonally averaged circulation of the middle atmosphere. *J. Atmos. Sci.* **35,** 577–591.

Simmons, A. J. (1974). Baroclinic instability at the winter stratopause. *Quart. J. Roy. Meteor. Soc.* **100,** 531–540.

Simmons, A. J., and Hoskins, B. J. (1980). Barotropic influences on the growth and decay of nonlinear baroclinic waves. *J. Atmos. Sci.* **37,** 1679–1684.

Smagorinsky, J. (1963). General circulation experiments with the primitive equations. 1. The basic experiment. *Mon. Weather Rev.* **91,** 99–164.

Smagorinsky, J. (1974). Global atmospheric modeling and the numerical simulation of climate. *In* "Weather and Climate Modification" (W. N. Hess, ed.), pp. 633–686. Wiley, New York.

Smagorinsky, J., Manabe, S., and Holloway, J. L. (1965). Numerical results from a nine-level general circulation model of the atmosphere. *Mon. Weather Rev.* **93,** 727–768.

Smith, B. A., Soderblom, L., and 25 co-authors (1981). Encounter with Saturn: Voyager 1 imaging science results. *Science* **212,** 163–191.

Smith, B. A., Soderblom, L., and 27 co-authors (1982). A new look at the Saturn system: The Voyager 2 images. *Science* **215,** 504–537.

Solberg, H. G. (1969). A three-month oscillation in the longitude of Jupiter's Red Spot. *Planet. Space Sci.* **17,** 1573–1580.

Sromovsky, L. A. *et al.* (1981). Implications of Titan's north–south brightness asymmetry. *Nature (London)* **292,** 698–702.

Sromovsky, L. A., Revercomb, H. E., Krauss, R. J., and Suomi, V. E. (1983). Voyager 2 observations of Saturn's northern midlatitude cloud features: Morphology, motions and evolution. *JGR, J. Geophys. Res.* **88,** 8650–8666.

Steinberg, H. L. (1973). Numerical simulation of quasi-geostrophic turbulence. *Tellus* **25,** 233–246.

Stevenson, D. J. (1982). Interiors of the giant planets. *Annu. Rev. Earth Planet. Sci.* **10,** 257–295.

Stommel, H., and Schott, F. (1977). The beta spiral and the determination of the absolute velocity field from hydrographic station data. *Deep-Sea Res.* **24,** 325–329.

Stone, P. H. (1973). The dynamics of the atmospheres of the major planets. *Space Sci. Rev.* **14,** 444–459.

Stone, P. H. (1976). The meteorology of the Jovian atmosphere. *In* "Jupiter" (T. Gehrels, ed.), pp. 586–618. Univ. Arizona Press, Tucson, Arizona.

Trafton, L. (1981). The atmospheres of the outer planets and satellites. *Rev. Geophys. and Space Phys.* **19,** 43–89.

Weidenschilling, S. J., and Lewis, J. S. (1973). Atmospheric and cloud structures of the Jovian planets. *Icarus* **20,** 465–476.

Whitehead, J. A. (1972). Observations of rapid mean flow produced in mercury by a moving heater. *Geophys. Fluid. Dyn.* **3,** 161–180.

Williams, G. P. (1975a). Some ocean-Jupiter connections. *Mode News,* No. 78, 1–4.

Williams, G. P. (1975b). Jupiter's atmospheric circulation. *Nature (London)* **257,** 778.

Williams, G. P. (1978). Planetary circulations: 1. Barotropic representation of Jovian and terrestrial turbulence. *J. Atmos. Sci.* **35,** 1399–1426.

Williams, G. P. (1979a). Planetary circulations: 2. The Jovian quasi-geostrophic regime. *J. Atmos. Sci.* **36,** 932–968.

Williams, G. P. (1979b). Planetary circulations: 3. The terrestrial quasi-geostrophic regime. *J. Atmos. Sci.* **36,** 1409–1435.

Williams, G. P. (1985). Geostrophic regimes on a sphere and a beta plane. *J. Atmos. Sci.* **42,** 1237–1243.

Williams, G. P., and Holloway, J. L. (1982). The range and unity of planetary circulations. *Nature (London)* **297,** 295–299.

Williams, G. P., and Holloway, J. L. (1985). Global circulations. *J. Atmos. Sci.* (in press).

Williams, G. P., and Yamagata, T. (1984). Geostrophic regimes, intermediate solitary vortices and Jovian eddies. *J. Atmos. Sci.* **41,** 453–478.

Williams, G. P., and Wilson, R. J. (1985). Rossby vortices, solitons and turbulence. *J. Atmos. Sci.* (in press).

Yamagata, T. (1976). Stability of planetary waves in a two-layer system. *J. Oceanog. Soc. Japan* **32,** 116–127.

Yamagata, T. (1977). Stability of planetary waves in a two-layer system (small M limit). *J. Met. Soc. Japan* **55,** 240–247.

Yamagata, T., and Kono, J. (1976). On energy and enstrophy transfer in two-dimensional non-divergent waves on a beta-plane. *J. Met. Soc. Japan* **54,** 454–456.

Yeh, T.-C. (1949). On energy dispersion in the atmosphere. *J. Meteorol.* **6,** 1–16.